5

Intraseasonal variability

Duane E. Waliser

5.1 INTRODUCTION

While the defining variability of a monsoon system is its seasonal character, its variability about its typical seasonal evolution is often of most interest and importance. In the case of the Asian and Australian summer monsoons, their intraseasonal character is especially prominent and unique. Figure 5.1 compares annual rainfall variability along with the interannual and intraseasonal variability (ISV) for the northern and southern hemisphere summer seasons. The annual standard deviation exhibits strong variability on either side of the equator, which is a depiction of the annual meridional migration of the tropical rainfall band – a fundamental manifestation of the monsoon. The maps of interannual variability, particularly that for boreal winter, emphasize the connection to El Niño/Southern Oscillation (ENSO)-related sea surface temperature (SST) variability in the tropical Pacific Ocean. These maps of ISV illustrate two important features. First, the intraseasonal rainfall variability is as large or larger than the variability associated with the other timescales illustrated. Second, it tends to be relatively most prominent in the Asian and Australian monsoon sectors. The time series in Figure 5.2 show the annual cycle of rainfall and the anomalous evolution of unfiltered and filtered rainfall over India and northern Australia for a sample of three years. These time series emphasize the overall dominance, apart from the annual variation, of the intraseasonal timescale on these monsoon systems, including its obvious role in dictating onset and break phases. Even from these simple diagnostic figures, it is evident that ISV is a fundamental component of these monsoon systems.

The material in this chapter is devoted to describing the ISV associated with the Asian, and to some extent the Australian, summer monsoon. This includes the role it plays in the monsoons' onsets and breaks, its seasonal evolution, its interannual and decadal variability, and remote influences. In addition, the chapter will discuss what is understood regarding the important physical processes associated with monsoon

B. Wang (ed.), *The Asian Monsoon*.

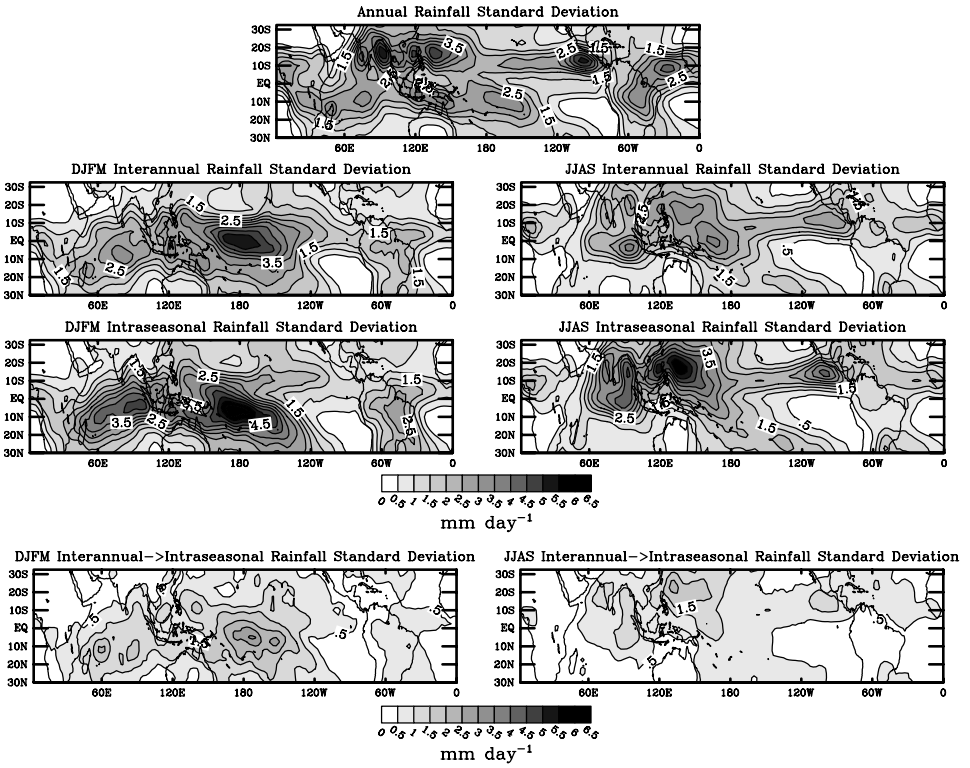

Figure 5.1. (*upper set of panels*) Rainfall variability maps for the global tropics. Rainfall data is based on pentad values of the satellite and *in situ* merged CMAP product of Xie and Arkin (1997) from 1979–1999. (*upper*) Annual cycle. In this case, the mean 73-pentad annual cycle was constructed from the data and the variance was computed about the annual mean; values shown in terms of standard deviation. (*middle*) Interannual variability. In this case, the data were low-pass filtered, retaining periods longer than 90 days. The variance of these interannual anomalies was computed for the December–March (*left*) and June–September (*right*) periods separately; values shown in terms of standard deviation. (*lower*) ISV. In this case, the data were band-pass filtered, retaining periods between 30 and 90 days. The variance of these intraseasonal anomalies was computed for the December–March (*left*) and June–September (*right*) periods separately; values shown in terms of standard deviation. (*lower set of panels*) Interannual variation of intraseasonal rainfall variability. In this case, the data were band-pass filtered, retaining periods between 30 and 90 days. The variance of these intraseasonal anomalies was computed separately for the December–March (DJFM; *left*) and June–September (JJAS; *right*) period. The variance of these values ($N = 21$ (20) for JJAS (DJFM)) was computed and is illustrated in terms of standard deviation.

ISV as well as our present capabilities and shortcomings in simulating and predicting it. While this book as a whole is devoted to the Asian monsoon, the treatment of ISV cannot be readily isolated to the boreal summer alone. The scientific developments associated with tropical ISV, including the observational and theoretical under-

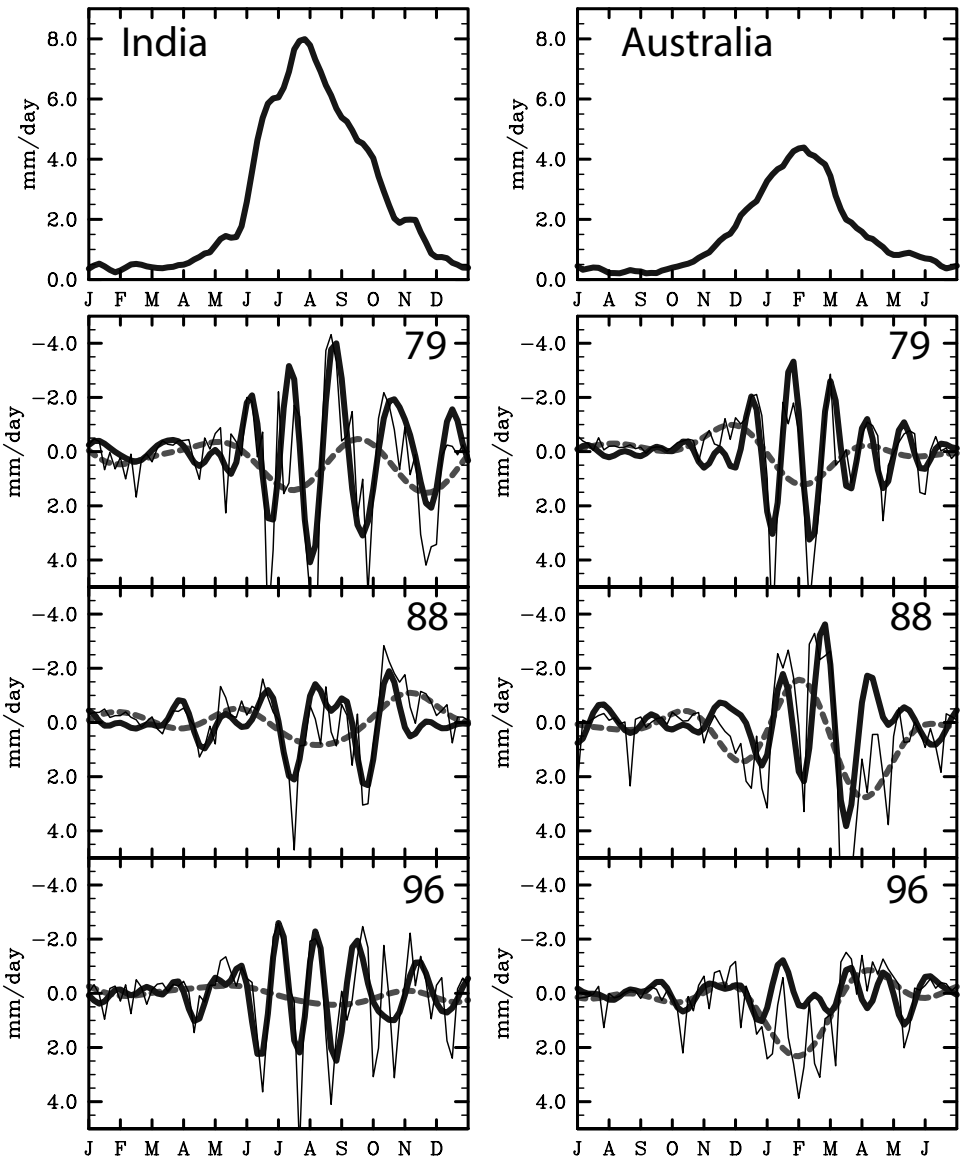

Figure 5.2. Time series of rainfall over India (*left*) and Australia (*right*). Rainfall data is based on pentad values of the satellite and *in situ* merged CMAP products of Xie and Arkin (1997) from 1979–1999. The data plotted for India (Australia) are the domain averages of the grid points lying within India (Australia, lying north of 25°S). (*top*) Mean 73-pentad annual cycle. (*lower three panels*) The thin black lines are pentad anomaly values, the thick black lines are 30–90-day band-passed values, and the thick dashed lines are 90-day low-pass values for the years 1979, 1988, and 1996.

pinnings as well as process-oriented modeling studies, have drawn from parallel, related, and/or comprehensive studies on both boreal summer and boreal winter manifestations. For this reason, much of this chapter necessarily involves review material associated with boreal summer (e.g., Asian summer monsoon) and boreal winter (e.g., Australian summer monsoon). Where possible and appropriate, the discussion is more tightly isolated to the Asian summer monsoon alone (e.g., 10–30-day variability, climatological intraseasonal oscillation (ISO), teleconnections). Note that more thorough reviews of a number of the topics discussed in this chapter can be found in Lau and Waliser (2005).

5.2 GENERAL DESCRIPTION

5.2.1 Madden–Julian Oscillation

Despite over a century of interest and study of the interannual component of the Asian monsoon (e.g., Blanford, 1884; Walker, 1923, 1924, 1928; Walker and Bliss, 1932; Walker, 1933; Banerji, 1950; Normand, 1953; Jagannathan, 1960; Banerjee *et al.*, 1978; Kung and Sharif, 1980, 1982; Shukla and Paolino, 1983; Mooley *et al.*, 1986; Hastenrath, 1987b; Shukla and Mooley, 1987; Parthasarathy *et al.*, 1988; Thapliyal and Kulshrestha, 1992; Webster and Yang, 1992; Parthasarathy *et al.*, 1994; Krishna Kumar *et al.*, 1995; Rajeevan *et al.*, 1998; Webster *et al.*, 1998; Gadgil *et al.*, 2002b; Gadgil, 2003; see also Chapter 6), the prominence of an organized intraseasonal component has only been recognized for about the last three decades. One of the first steps in this recognition came in the early 1970s with the discovery of an intraseasonal 'oscillation' in the tropics, that has since been named the Madden-Julian Oscillation (MJO; also known as the 30–60-day, 40–50-day, and tropical intraseasonal oscillation) after its discoverers (Madden and Julian, 1971). These 'oscillations' were initially detected in tropical wind and surface pressure data from available radiosonde and station data. Considering the data and computational resources available at the time, this discovery was quite remarkable. A historical perspective of this discovery can be found in Madden and Julian (2005). Subsequent to its initial detection in station data, the MJO was soon after detected in satellite observed brightness temperature/cloudiness data (Gruber, 1974; Zangvil, 1975) and has since been characterized by a number of further observational studies, a review of which can be found in Madden and Julian (1994). An additional, more recent review of the MJO as it pertains to the Australian–Indonesian monsoon can be found in Wheeler and McBride (2005).

Figure 5.3 illustrates the canonical space–time structure of an MJO event using a composite analysis of contemporary data sources. The rainfall maps illustrate its eastward propagation and equatorially trapped character. Comparison of the upper and lower tropical wind fields emphasize the baroclinic nature of its wind anomalies. In addition, it can be seen that the MJO has a global scale with wind anomalies, particularly at upper levels, being primarily characterized by wavenumber 1, and with rain and low-level winds being primarily characterized by wavenumber 2 –

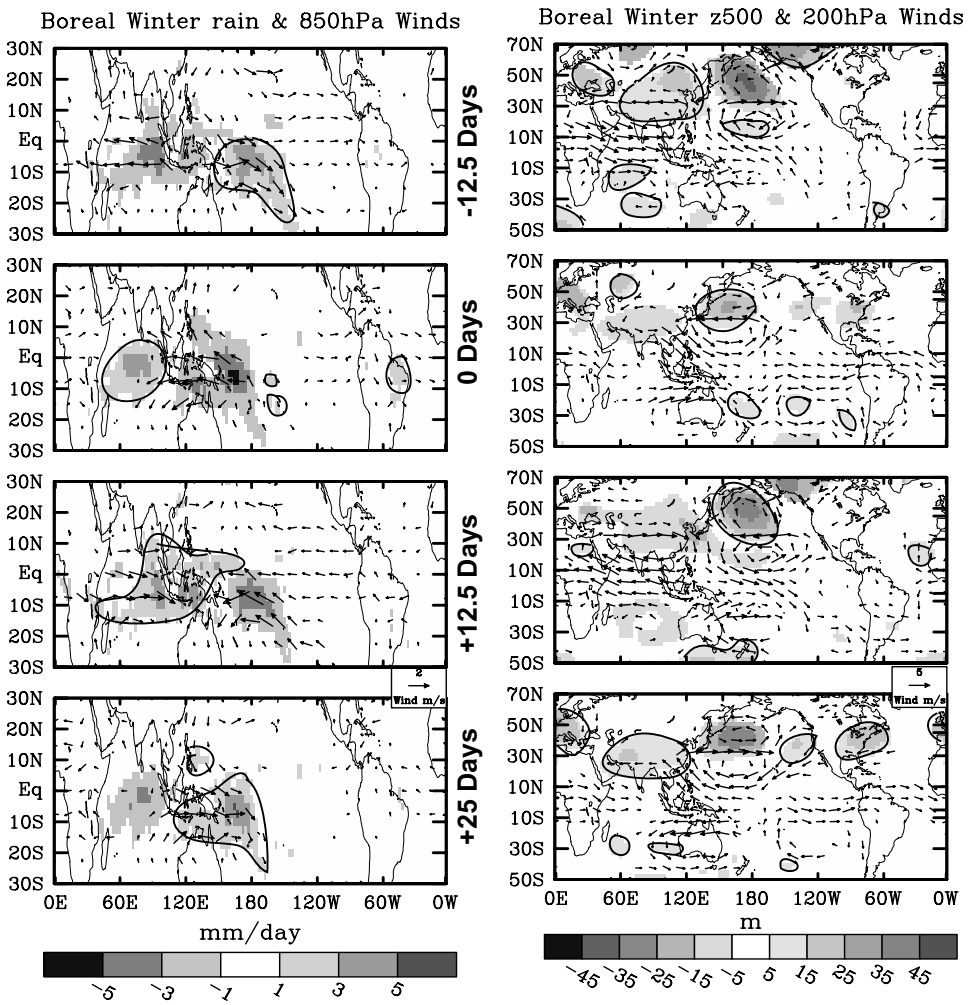

Figure 5.3. Canonical structure of an MJO event based on 5-day average (i.e., pentad) NCEP/NCAR Reanalysis (Kalnay *et al*., 1996) and CMAP rainfall data (Xie and Arkin, 1997) from 1979–2000. Data were band-pass filtered with a 30–90-day filter and then separated into boreal winter (November–April) and summer (May–October). Extended EOF (EEOF) analysis with ±5 pentad lags was performed on tropical rainfall (30°N–30°S, 30°E–180°E) to identify the dominant 'mode' for the winter and summer separately. Composite events were constructed by selecting events if the EEOF amplitude time series exceeded 1 standard deviation ($N = 43$ (49) for winter (summer)). The resulting composites have dimensions lag (−5 to +5 pentads), latitude, and longitude. In the plots above, only 4 panels of the boreal winter composite are shown, each separated by 2.5 pentads (i.e., 12.5 days). Plots on the left show composite rainfall and 850-hPa wind vectors between 30°N and 30°S. Plots on the right show 500-hPa geopotential heights and 200-hPa wind vectors between 70°N and 50°S. Only values that exceed the 90% confidence limit are shown. Positive anomalies are encircled by a single countour.

although modulated by the relatively warmer (cooler) eastern (western) hemisphere background state. For example, over the Indian and west Pacific Oceans, there is evidence of considerable interaction between the wind and rainfall anomalies. In these regions, where the coupling between the convection and warm surface waters is strong, the oscillation propagates rather slowly, about 5–10 $m\,s^{-1}$. However, once the disturbances reach the vicinity of the Date Line, and thus cooler eastern Pacific Ocean equatorial waters, the convection tends to subside and propagate south-eastward into the South Pacific convergence zone (SPCZ). Beyond the Date Line, the disturbance is primarily evident only in the wind field with characteristics similar to a dry Kelvin wave with a speed of about 15–20 $m\,s^{-1}$ or greater (e.g., Hendon and Salby, 1994).

Another important feature associated with the MJO, especially in relation to its connections to mid-latitudes and its connections to the boreal summer ISO, is its off-equatorial structure and variability. From Figure 5.3 there is evidence of off-equatorial Rossby wave gyres that straddle the near-equatorial rainfall anomalies. For example, in the composite maps at lag +12.5 days, the positive rainfall (i.e., heating) anomaly is located over the Maritime Continent. Associated with this are upper level cyclonic (anticyclonic) gyres to the north-east and south-east (north-west and south-west) centered at latitudes of about 20°. These gyres are easily identified in the maps of the MJO life cycle constructed by Hendon and Salby (1994) and are consistent with the circulation that is expected in association with a near-equatorial tropospheric heating anomaly (Matsuno, 1966; Gill, 1980). One of the important manifestations of these tropical heating and subtropical streamfunction anomalies is that they act as Rossby wave sources for mid-latitude variability (e.g., Weickmann, 1983; Liebmann and Hartmann, 1984; Weickmann *et al.*, 1985; Lau and Phillips, 1986; Sardeshmukh and Hoskins, 1988; Berbery and Noguespaegle, 1993). For example, the +12.5-day lag map of Figure 5.3 shows evidence of a wave train emanating from the tropics and extending poleward and eastward over the Pacific Ocean and North America. Such connections with the extratropics have important ramifications for mid-latitude weather variability, regime changes, and forecasting capabilities (e.g., Ferranti *et al.*, 1990; Higgins *et al.*, 2000; Jones *et al.*, 2004a).

The ISV characteristics discussed above tend to be most strongly exhibited during the boreal winter and spring when the Indo–Pacific warm pool is centered at or near the equator. From the rainfall maps in Figure 5.3, it is evident that the MJO has its greatest impact on Australian monsoon rainfall variability (e.g., right panels of Figure 5.2). However, as will become evident the principal mode of ISV that influences the Asian summer monsoon shares many of the same properties, and in large part their differences derive mainly from a consideration of the seasonal modulation of ISV. There have been a number of terminologies applied to the boreal summer ISO, ranging from simply ISO, monsoon ISO (MISO), and even just the MJO, where the latter simply takes the viewpoint that there is one inherent phenomenon modulated by the annual cycle. In this chapter, it is important to be able to distinguish the two different phenomena (or, if one prefers, the seasonal modulation of the phenomenon) and their associated research developments. Thus the form of ISV that most directly affects the Asian summer monsoon, and in this sense is

different from the MJO form of ISV that primarily affects the Australian summer monsoon, will be referred to as the boreal summer ISO or just the ISO.

5.2.2 Boreal summer ISO

Beginning around the mid to late 1970s, a number of studies began to identify intraseasonal fluctuations, with periods around 40–50 days, associated with the Asian summer monsoon. These included analysis of both cloudiness (Murakami, 1976a; Yasunari, 1979, 1980) and wind variability (Dakshinarmuti and Keshavamurty, 1976; Murakami, 1977). These initial studies set the stage, and in essence primed the community, for a very active research period on the ISO that was forthcoming in association with the First GARP (Global Atmospheric Research Program) Global Experiment (FGGE) in 1979 (NA, 1978; Fleming *et al.*, 1979). In hindsight, the FGGE year could not have turned out better in terms of providing an ideal data set for carrying out ISO-related monsoon research. For example, examination of the Indian rainfall plots such as those in Figure 5.2 for all years since 1979 illustrate that the 1979 summer had one of the most robust ISV signatures of any year since. The resulting enhanced data set from the FGGE provided the observational resources for a multitude of ISO-related studies (e.g., Lorenc, 1984; Krishnamurti and Gadgil, 1985; Murakami and Nakazawa, 1985; Cadet, 1986; Chen, 1987; Murakami, 1987a; Krishnamurti *et al.*, 1988; Krishnamurti *et al.*, 1990; Chen and Yen, 1991; Krishnamurti *et al.*, 1992a; Chen and Chen, 1993; Chen and Chen, 1995).

Figure 5.4 illustrates the canonical space–time structure of a typical boreal summer ISO event using a composite analysis of contemporary data sources (see among others, Krishnamurti and Subrahmanyam, 1982; Chen and Murakami, 1988; Goswami *et al.*, 1998; Annamalai *et al.*, 1999; Annamalai and Slingo, 2001; Hsu and Weng, 2001; Kemball-Cook and Wang, 2001; Lawrence and Webster, 2002; Hsu *et al.*, 2004). The rainfall map at lag 0 days shows that positive rainfall anomalies in the western and central Indian Ocean occur in conjunction with negative rainfall anomalies over a region extending between India and the western equatorial Pacific. This system then appears to propagate in both an eastward and northward fashion. Examination of the near-equatorial region alone gives the impression of an MJO-like phenomenon described above, although more confined in longitude. On the other hand, examination of a given longitude sector anywhere between 80°E and 130°E gives the impression of a northward-propagating phenomena (e.g., Figure 5.15, p. 239). Studies such as those by Yasunari (1979) and Lau and Chan (1986) tied these two different aspects of propagation together and pointed out the comprehensive nature of the phenomena. From these figures, it is evident now that the intraseasonal variations in rainfall depicted in Figure 5.2 are closely associated with the type of space–time variability shown in Figure 5.4 (and Figure 5.15). These variations largely account for what are often referred to as 'active' and 'break' periods of the monsoon which, as discussed above, make up a critical feature of the Asian monsoon system and its variability (Blanford, 1886; Ramaswamy, 1962; Raghavan, 1973; Ramanadh *et al.*, 1973; Krishnamurti and Bhalme, 1976;

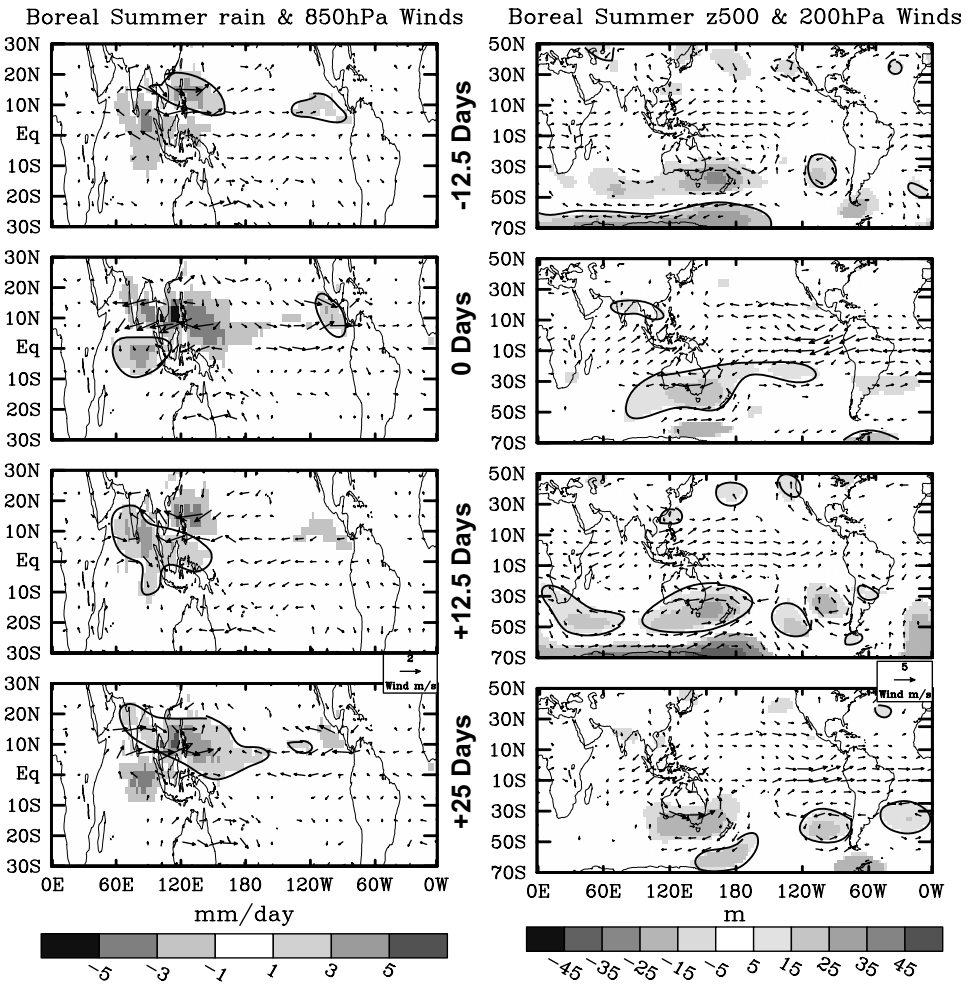

Figure 5.4. Same as Figure 5.3, except for boreal summer (May–October), and with the panels on the right extending from 50°N to 70°S.

Alexander *et al.*, 1978; Sikka, 1980; Cadet, 1983; Bhide *et al.*, 1997; Annamalai and Slingo, 2001; Gadgil, 2003; Gadgil and Joseph, 2003).

While the diagram in Figure 5.4 illustrates what might be considered a typical ISO event, it is important to recognize that these events have considerably more complexity in reality. For example, the study by Wang and Rui (1990a), and later by Jones *et al.* (2003), have further diagnosed the 'synoptic climatology' of tropical ISV events, including their seasonal modulation (see also Lawrence and Webster, 2002). Both studies used forms of convective (i.e., OLR) anomaly 'tracking', the former being more subjective and the latter an objective approach, to illustrate the typical pathways that ISV events follow. Viewed within this paradigm, each of the identified

categories of events would at some point within their eastward migration move northward into the Indian subcontinent or into south-east Asia and the western north Pacific Ocean. Apart from these types of variations, it is important to point out that there is a fair bit of variability even within the monsoon season when considering the nature of ISO events and the influence of the background state. For example, Figure 5.5 illustrates how the typical pattern of intraseasonal variance is modified over the course of the monsoon season (Kemball-Cook and Wang, 2001). During the onset month(s) of the monsoon, most of the variability occurs in the Indian sector while during the final month(s) of the monsoon, most of the variability occurs in the east Asian and western North Pacific sectors. This seasonal variation was shown to be consistent with the seasonal march of the warmest SSTs, which begin to develop in the northern Indian Ocean in the early monsoon period and eventually are found around south-east Asia and the north-western tropical Pacific in the later part of the summer.

With the above seasonal modulation in mind, Kemball-Cook and Wang (2001) produced a schematic of the synoptic evolution of an ISO event. This diagram is shown in Figure 5.6. It illustrates a mixture of the underlying wave characteristics, and their propagation features, associated with the space–time and variance structures shown in Figures 5.4 and 5.5. For both the early and late monsoon season, there is what can be considered an initiation phase in the equatorial Indian Ocean, an eastward propagating component, and a recurrent emission of Rossby waves. For the initiation phase, the main difference between early and late summer, is that during late summer there is an eastward displacement of the location of the initiation phase. For the eastward propagating component, the main difference is that in late summer, the propagation appears to be somewhat discontinuous and 'jumps' across the Maritime Continent. In addition, there is less latitudinal symmetry in late summer, as warm moist surface conditions have moved mostly to the north of the equator.

The off-equatorial disturbances shown in Figure 5.6 are associated with the emanation of Rossby waves from the near-equatorial convection anomaly. It is this feature that makes the propagating characteristics of the boreal summer ISO particularly complex. These disturbances are associated with three directions of propagation. Considered in isolation, they have an inherent westward propagation (Matsuno, 1966). This accounts for some aspects of the westward propagating variability that is found, particularly in the latter part of the summer, in the south-east Asian sector/western North Pacific Ocean and/or that is associated with higher frequency ISV that will be discussed in more detail below. On the other hand, the emanation of these Rossby waves occurs from a very large-scale, eastward-moving, near-equatorial convective anomaly (e.g., Lawrence and Webster, 2002). Finally, there are physical processes that promote northward propagation of these Rossby wave disturbances that will be discussed in Section 5.5. Considering these latter two aspects together, largely accounts for the appearance of the eastward-propagating, north-west–south-east tilted, large-scale 'rain band' evident in Figure 5.4. Note that in some constructions this 'tilted rain band' appears more like a quadrapole feature (e.g., Annamalai and Slingo, 2001). Kemball-Cook and

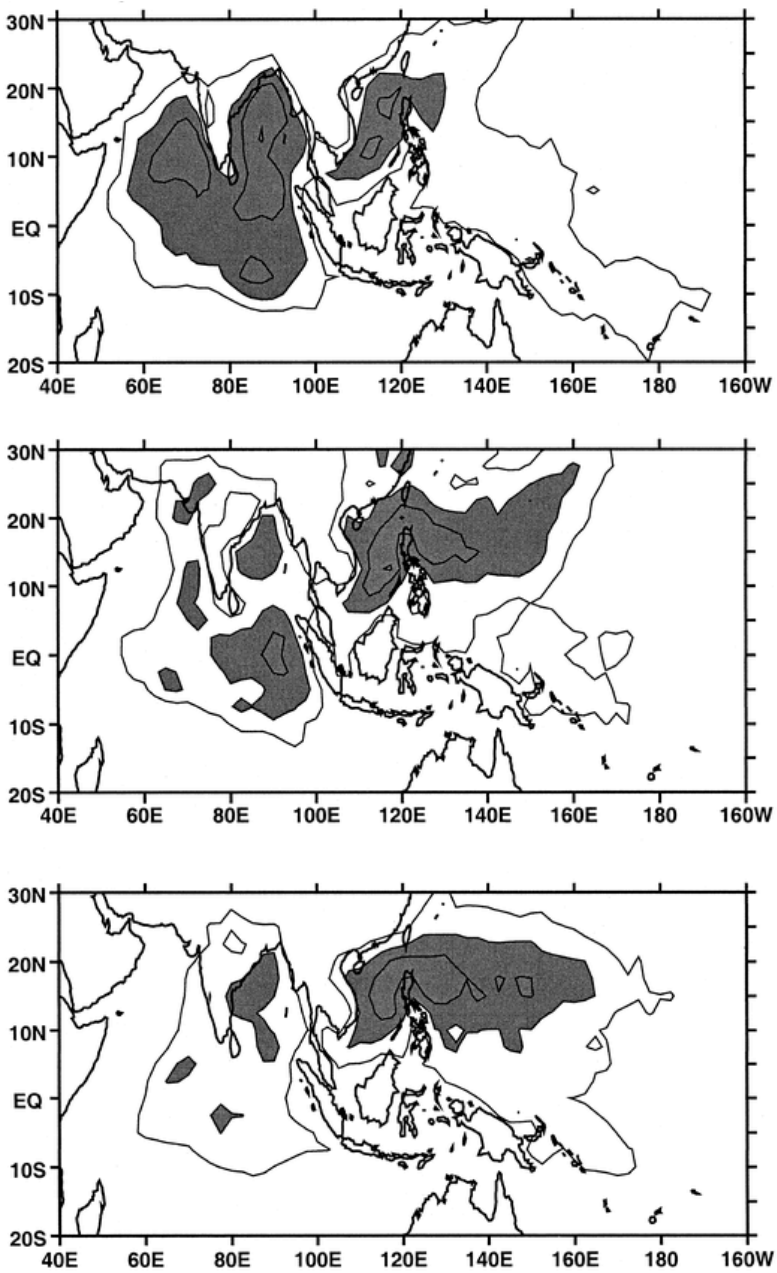

Figure 5.5. Seasonal variation of 10–100-day filtered OLR variance. (*top*) May–June average, (*middle*) July average, and (*bottom*) August–October average. Contour interval is 250 $(\mathrm{W\,m^{-2}})^2$. First contour at 500 $(\mathrm{W\,m^{-2}})^2$. Regions where the OLR variance >750 $(\mathrm{W\,m^{-2}})^2$ are shaded.
From Kemball-Cook and Wang (2001).

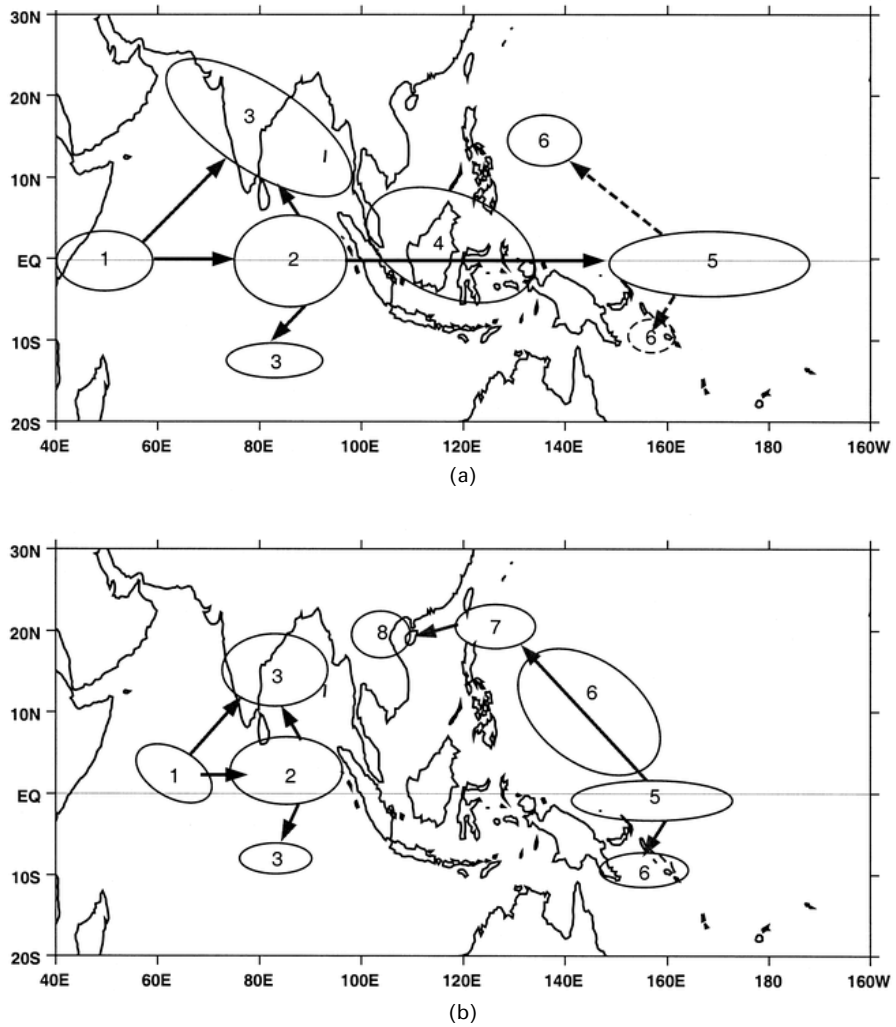

Figure 5.6. Boreal summer ISO convection life cycle for (a) May–June and (b) August–October. Ovals indicate convection, with numbers indicating the evolution of the anomaly. Horizontal arrows indicate eastward propagation of convection along or near the equator. Vertical/slanted arrows indicate poleward propagation of convection due to emanation of Rossby waves from equatorial convection. Dashed lines indicate a low-amplitude signal. From Kemball-Cook and Wang (2001).

Wang (2001) pointed out that north–south asymmetry and the enhancement of this Rossby wave component in the latter part of the monsoon season are associated with the change in the background state (e.g., SST and surface moisture) and accompanying enhancements in the large-scale easterly vertical shear (Li and Wang, 1994; Wang and Xie, 1996, 1997). For additional and more thorough reviews of the boreal summer ISO, the reader is referred to Goswami (2005) and Hsu (2005).

5.2.3 High-frequency ISV

In addition to the prevalence of ISV with a nominal timescale of 40–60 days, there is also considerable ISV at higher frequencies, at timescales of around 10–20 days. Detection of these higher frequency fluctuations came from early studies on cloudiness and conventional synoptic observations (Krishnamurti and Bhalme, 1976; Murakami, 1976b; Yasunari, 1979; Krishnamurti and Ardanuy, 1980). However, it wasn't until the 1980s and even the 1990s that enough data became available to more thoroughly document the temporal and spatial structure as well as the modulation of the variability over the course of the monsoon season (Lau *et al.*, 1988a; Tanaka, 1992; Chen and Chen, 1993; Fukutomi and Yasunari, 1999; Chen *et al.*, 2000; Annamalai and Slingo, 2001; Hsu and Weng, 2001). For example, Figure 5.7 shows Annamalai and Slingo's depiction of the 10–20-day mode calculated from 10–20-day band-passed OLR data using Principal Oscillation Pattern (POP; Hasselmann, 1988) analysis. This mode accounted for about 1/4 of the subseasonal monsoon variability while the 30–60-day (i.e., ISO) accounted for about 2/3. In contrast to the lower frequency ISO, this mode's variability is focused almost entirely over east Asia and the north-west tropical Pacific region. Moreover, their analysis indicates that in contrast to the 30–60-day mode, whose large-scale structure appears to originate in the equatorial Indian Ocean and propagate northward/north-eastward, the 10–20-day mode originates in the equatorial western Pacific and propagates westward/north-westward in the form of Rossby waves at about $5\,\mathrm{m\,s^{-1}}$.

Based on the studies noted above, another noteworthy feature of the 10–20-day mode is that it has a relatively strong seasonal variation. In particular, during the early summer monsoon period (e.g., May–July), there is considerable 30–60-day variability exhibited at and near the equator and in particular in the Indian sector, with relatively little 10–20-day variability evident. However, as the monsoon season progresses, the focal point of the 30–60-day variability moves north-eastward (Figure 5.5) with strong 10–20-day variability developing in the east Asian and north-western tropical Pacific Ocean. The concurrence of high amounts of 30–60 and 10–20-day variability in this region during the latter half of the monsoon makes this period and region of the monsoon particularly challenging to diagnose, understand, and model. More generally, the role of the 10–20-day variability in determining or modulating monsoon onset breaks, either separately or in conjunction with 30–60-day variability, is still an outstanding question.

As there have been less observational studies of the 10–20-day variability compared with the 30–60-day ISO mode, there have also been fewer hypotheses as to its origin. Krishnamurti and Bhalme (1976) suggested the 10–20-day mode could arise from a cloud–radiation–convective feedback. While plausible, there was no quantitative support provided for a selection of the given timescale and none for the overall spatial structure – which was probably not that well defined at the time. Goswami and Mathew (1994) invoked an evaporation–wind feedback (see Section 5.5) to describe the instability but their most unstable mode had a zonal wavelength of about $9\text{–}12 \times 10^3$ km which is significantly larger than the $5\text{–}6 \times 10^3$ km wavelength evident in Figure 5.7. Recently, Chatterjee and Goswami (2004) used a

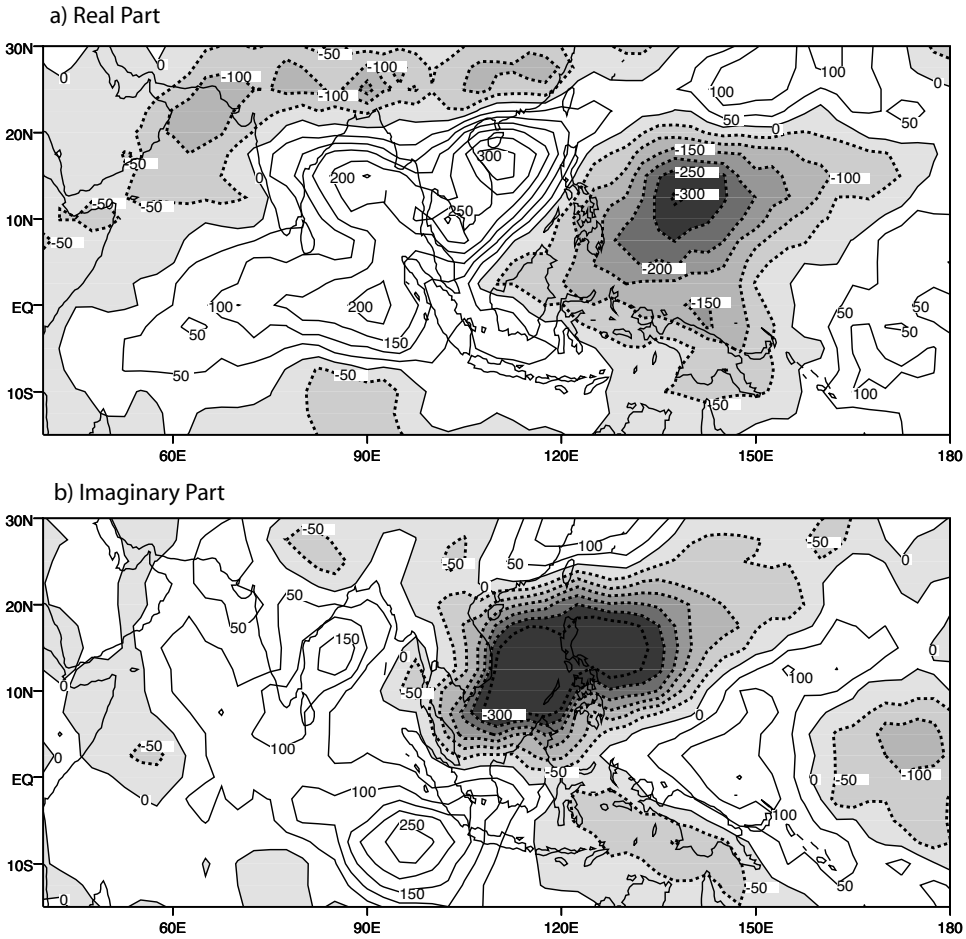

Figure 5.7. Real and imaginary POPs for an analysis of 10–20-day band-pass filtered OLR data. The rotation period of the POP is 17 days and the decay time is 20 days. The contour interval is 50 and the shading denotes negative values. Taken together, these two patterns depict an westward/north-westward propagating oscillation.
From Annamali and Slingo (2001).

simplified 2-layer atmospheric model coupled to a steady Ekman boundary layer to examine the nature of the 10–20-day mode (referred to as the quasibiweekly mode; QBM). Their model results suggest that the QBM is an $n = 1$ Rossby wave which is modified by the mean background state. The latter provides for the 'dynamic equator', and thus the Rossby wave itself, to be displaced northward giving the modal structure of the pattern more consistency with the observations. The source of instability comes from the interaction between convective heating and frictional moisture convergence within the (off-equatorial) region of low-level vorticity.

5.2.4 Climatological ISO

While Figure 5.2 suggests a fair amount of year-to-year variability in the character of the monsoon's ISO variability (discussed in more detail in Section 5.4), there is actually enough year-to-year similarity to make up what has been termed the 'climatological ISO' (CISO; after Wang and Xu, 1997). This feature has been detected and examined by a number of studies (Lau *et al.*, 1988a; Kang *et al.*, 1989; Nakazawa, 1992; Wang and Xu, 1997; Kang *et al.*, 1999) and is illustrated in the time–latitude diagrams constructed by Kang *et al.* (1999) that are shown in Figure 5.8. In each case, long-term average (~5 summers) values of pentad cloud fraction is shown. These diagrams illustrate that the mean evolution of the monsoon

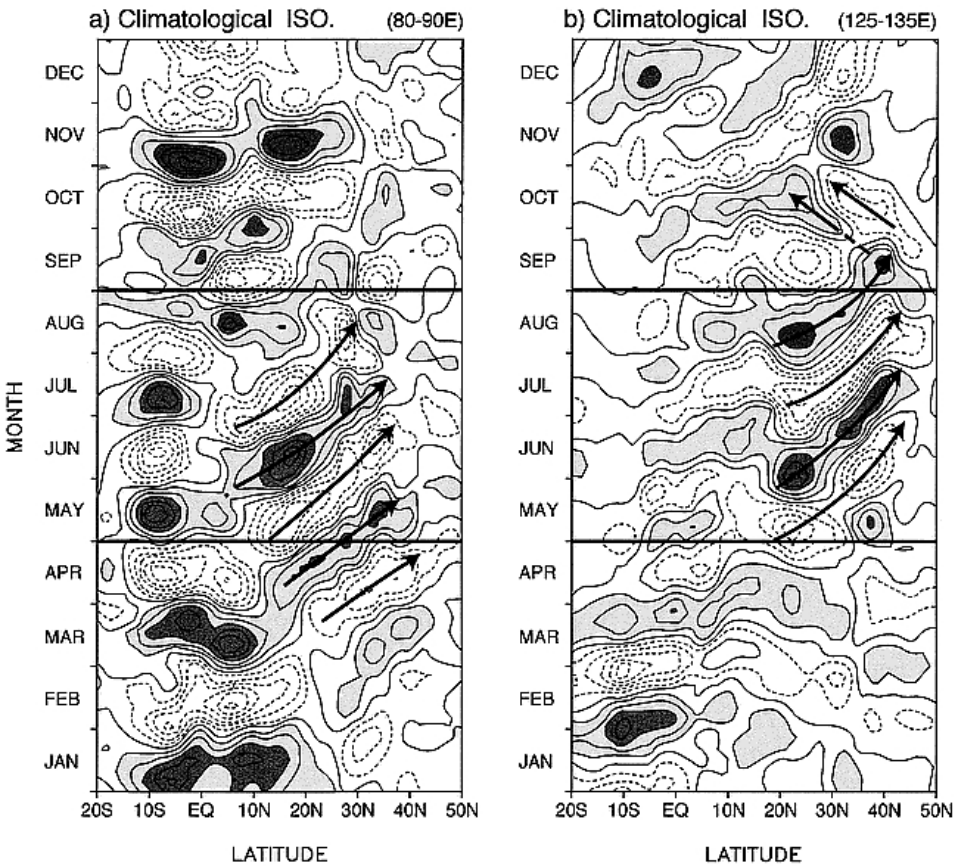

Figure 5.8. Hovmoeller diagrams of climatological intraseasonal component of cloud fraction along longitudinal bands of (a) 80°–90°E and (b) 125°–135°E. Contour interval is 0.02. Light and dark shading indicates the cloud fractions between 0.02 and 0.06 and those greater than 0.06, respectively.
From Kang *et al.* (1999).

exhibits structured (northward) propagation characteristics similar to the 'synoptic' ISO events described above. While the number of years used in their analysis is relatively few to ensure statistical significance, the analysis of Wang and Xu (1997) uses 17 years of OLR to illustrate that the subseasonal variability (i.e., CISOs) exhibited in the mean climatology is distinct from its smooth seasonal evolution.

The above line of research has helped support, and dovetailed with, a parallel line of research that has over the years discussed the multistage onset of the Asian summer monsoon, particularly in the south-east Asian region (e.g., Ding, 1992; Matsumoto, 1992; Tanaka, 1992; Ueda *et al.*, 1995; Wu and Wang, 2001; Wang and LinHo, 2002). For example, the northward propagation of the climatological convection that begins in mid-May (Figure 5.8) is associated with the monsoon onset in the South China Sea region and then subsequently in mid June the onset of the Meiyu in Central China and the Baiu in Japan. By this time, the South China Sea region is undergoing a climatological withdrawal, which subsequently happens in central China and Japan as the convective signal moves further north ($\sim 40^{\circ}$). By around early August, there is a return of active conditions around 20°N and another northward propagating climatological feature. While the CISO provides a framework for understanding, and even predicting, regional monsoon onset characteristics, it should be emphasized that just as the ISO might be considered a fundamental building block of the climatological onset, it can also produce a fair amount of variability to the onset and even be responsible for delaying or producing false onsets (Flatau *et al.*, 2001; Flatau *et al.*, 2003).

5.3 SYNOPTIC ORGANIZATION AND REMOTE INFLUENCES

The subseasonal time and planetary spatial scales of the boreal summer ISO give it the means to modulate synoptic activity at considerably smaller time and space scales as well as the circulation in regions remote from the main convective disturbances. This section briefly examines a number of interactions of this sort, including both local and remote organization of tropical storm activity. While a number of studies have noted a modulation of synoptic activity such as tropical storms by ISV in the Indian sector (Yasunari, 1981; Murakami *et al.*, 1986; Liebmann *et al.*, 1994), Goswami *et al.* (2003) have performed a recent analysis for the period 1954–1993 with very clear demonstrable results pertaining to the Indian monsoon. Their analysis focused on the development and subsequent tracks of low-pressure systems (i.e., lows and depressions; LPS). They first developed an ISO index based on filtered 850-hPa relative vorticity. Then they plotted the genesis and track information for the LPS that occurred within what they referred to as the 'active' and 'break' phases of the ISO (analogous to the 4th and 2nd panels of Figure 5.4, respectively); their results are shown in Figure 5.9. In the active phase, there is a strong preference for the development of LPS to occur in what amounts to the seasonal mean position of the monsoon trough and region of maximum relative vorticity (Chapters 2, 4, and 9), both of which are accentuated during the 'active' phase of the ISO. In the break phase, there is a clear diminution of LPS

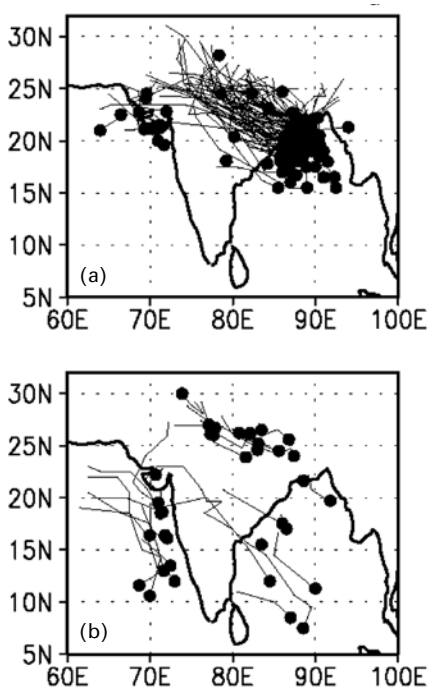

Figure 5.9. Tracks of LPS for the period 1954–1983 during extreme phases of the boreal summer ISO. (a) 'Active' ISO phase (analogous to the 4th panel of Figure 5.4) and (b) 'break' ISO phase (analogous to the 2nd panel of Figure 5.4). Dark dots represent the genesis point of the LPS and their lines show the tracks.
From Goswami *et al.* (2003).

development, with the few that do develop occurring on the northward and southward edges of the seasonal mean trough – regions where the ISO in the 'break' phase (as referred to here) is enhancing convective activity and low-level vorticity. They noted a 3.5 times increase in LPS development during the active vs. the break phase. Also noteworthy in their study was that they determined that this so-called 'clustering' of LPS activity was separately modulated by both 30–60-day and 10–20-day frequency bands in approximately equal amounts, and that the clustering was particularly strong when the enhancement effect from both bands acted on concert.

Along with the Indian sector, there is also significant evidence for synoptic modulation by ISV in the east Asian and north-western tropical Pacific Ocean. Many of the studies on this topic have been concerned with the modulation of tropical cyclones. As with the LPS results above, a number of studies have found that typhoons tend to develop in active monsoon trough regions (Harr and Elsberry, 1995; McBride, 1995). Since the location and spatial extent of the monsoon trough is strongly modulated by ISO activity, it is expected that modulations of typhoon activity occur in conjunction with the ISO. For example, Nakazawa (1986) found that during the FGGE year, tropical cyclones tended to occur in the convective

phases of the ISO, including both the 15–25 and 30–60-day variations. Curiously, prior to this, Gray (1978) found that tropical cyclone formation tended to cluster in 1–2 week periods with these periods being separated by 2–3 weeks. Clearly, Gray was seeing the effect of the ISO but had too little data to work with and as yet the ISO was just beginning to be detected and defined. Maloney and Dickinson (2003) performed a detailed analysis of the energetics of this relationship and found that when 850-hPa wind anomalies are westerly (i.e., the 4th panel of Figure 5.4), small-scale eddies tend to grow through barotropic eddy kinetic energy conversion from the mean flow. The development of these eddies, together with strong surface convergence and 850-mb cyclonic shear that occur in conjunction with this phase of the ISO (i.e., the 4th panel of Figure 5.4 between about 120°–150°E and about 5°–20°N), and the high mean sea surface temperatures during the late boreal summer, create the favorable environment for tropical cyclone formation. Along with the evidence for ISO modulation of tropical cyclones, there is also considerable evidence for the modulation of more generalized synoptic disturbances and wave activity in the east Asian and tropical west Pacific Ocean region (Nakazawa, 1986; Lau and Chan, 1988; Sui and Lau, 1992; Salby and Hendon, 1994; Hartmann and Maloney, 2001; Straub and Kiladis, 2003).

Just as noteworthy as the local modulation of tropical convective activity by ISO is evidence from a number of studies that such modulation can extend to a near global extent (Higgins *et al.*, 2000; Maloney and Hartmann, 2000a,b; Mo, 2000). These studies have each examined the downstream influence of the boreal summer ISO on tropical storm and/or hurricane development. For example, Maloney and Hartmann (2000a,b) found evidence that the ISO, through its effects on low-level winds in the eastern Pacific (see the 2nd and 4th panels of Figure 5.4) has a strong modulating effect on hurricane development in the eastern Pacific and Gulf of Mexico. Mo (2000) found that this influence extends to the tropical storm activity in the Atlantic. The study by Higgins *et al.* (2000) demonstrated the global nature of these influences by compositing the 200-hPa velocity potential anomalies for 21 strong ISO events between 1979 and 1997. Then as shown in Figure 5.10, they posted the point of origin of all tropical storms that developed into hurricanes/typhoons and that occurred during those 21 ISO events. Clearly evident is a robust, global-scale modulation by the ISO wavenumber one circulation anomaly that leads to an enhancement (suppression) of hurricane/typhoon formation in the rising (subsiding) branch of the anomalous circulation. The results described in this section, coupled with the potential predictability of the ISO itself, discussed in Section 5.7, provide a valuable means to possibly predict, on a regional scale, the occurrence of regimes when extreme tropical events are more or less likely to occur.

5.4 LOW-FREQUENCY VARIABILITY

It is evident from Figure 5.2 that the amount and character of the ISV associated with the Asian and Australian monsoon systems varies considerably from year to year. For example, as mentioned above, the 1979 FGGE year was characterized by

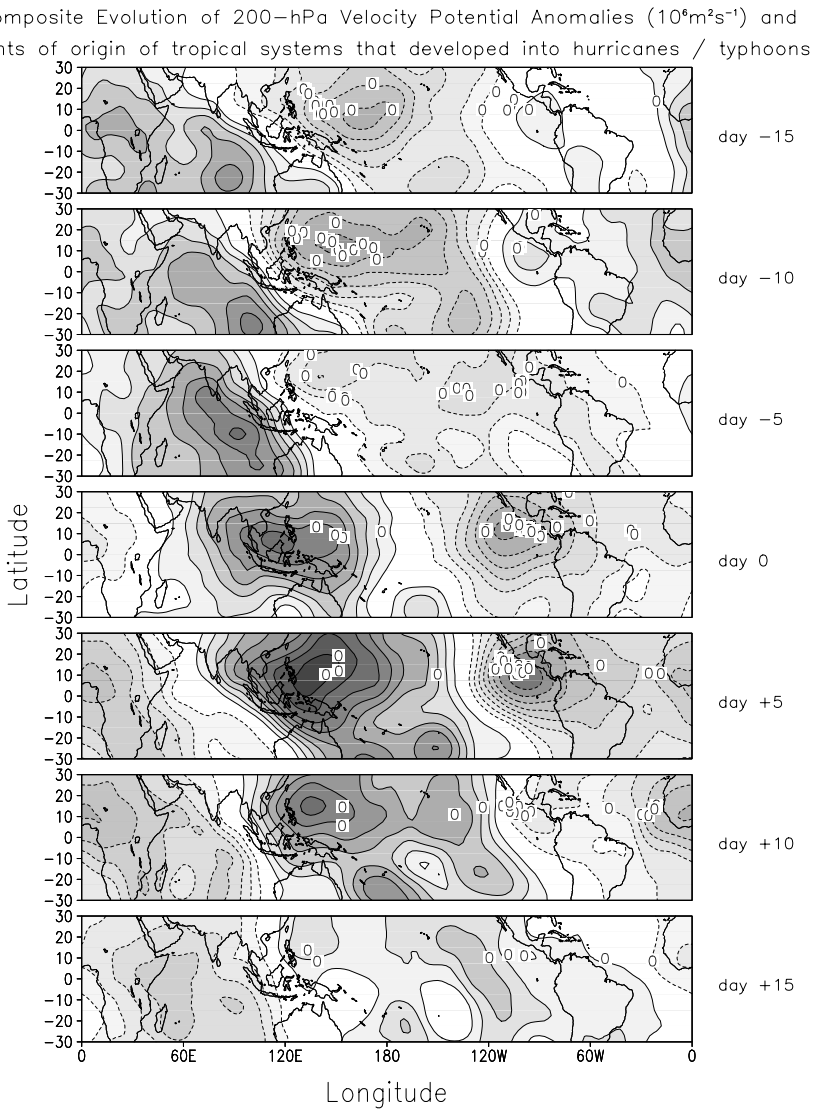

Figure 5.10. Composite evolution of 200-hPa velocity potential anomalies associated with the boreal summer ISO and points of origin of tropical systems that developed into hurricanes/typhoons. Note that panels 1–4 in Figure 5.4 roughly correspond to lags −5, +5, +15, and −15 days, respectively. The light (dark) shading roughly corresponds to regions where convection is favored (suppressed) as represented by 200-hPa velocity potential anomalies Composites are based on 21 ISO events, each considered over a 35-day period. Hurricane track data is for the period July–September for 1979–1997. Points of origin in each panel are for different storms – only those that occurred during the 21 selected ISO events. Contour interval is $0.5 \times 10^6\ \mathrm{m^2\ s^{-1}}$, negative contours are dashed, and the zero contour is omitted for clarity.
From Higgins *et al.* (2000).

very large and regular intraseasonal fluctuations in both the Indian and Australian summer monsoon sectors. On the other hand, 1988 exhibited rather weak ISV over India and rather typical variability over Australia, vice versa for 1996. The lower set of maps in Figure 5.1 quantify this variability by illustrating the amount of year-to-year variability associated with the intraseasonal variance presented in the upper set of panels. Specifically, the two intraseasonal maps in the upper set of plots in Figure 5.1 show the typical amount of intraseasonal rainfall variability in any given season, and the two lower maps show the interannual variability associated with this quantity. When considering these quantities in terms of variance (as opposed to standard deviation which is what is illustrated; see caption for details), the typical change from year to year is of the order of 30%. Thus, the variations are considerable and these have a profound impact on the year-to-year character of the summer monsoons. This section reviews the low-frequency variations of the ISV, namely the interannual variations (see Chapter 7 for decadal and interdecadal variations) as well as considerations of whether and how the ISV itself may produce a rectified signal onto the seasonal and/or interannual mean state.

5.4.1 Interannual variability

A number of observational studies have noted interannual variations of ISV in the observational record. Most of this research was initiated in association with the MJO (e.g., Lau and Chan, 1988; Salby and Hendon, 1994) although there have since been a substantial number of investigations involving the boreal summer ISO. These investigations have tended to fall into one of three categories: (1) determining what mechanisms are responsible for producing the observed interannual variability of ISV, (2) determining how the interannual variability in ISV might modulate the interannual character of the monsoon, and (3) understanding the degree that the interannual variations in ISV, primarily the MJO in this case, influence the development and evolution of interannual SST variability (e.g., ENSO). The first two of these are addressed in more detail below. The latter of the three lies beyond the scope of this chapter. However, recent summary and review discussions of this issue can be found in Zhang *et al.* (2001), Lau (2005), and Kessler (2005).

Figure 5.11 shows Hendon *et al.*'s (1999) illustration of the interannual variability of the MJO. These calculations are based on a number of different MJO indices. It shows for example that the winter/spring periods of 1984, 1989, and 1996 exhibited particularly pronounced MJO activity while the winter/spring periods 1975, 1982, and 1994 exhibited very weak MJO activity. Apart from the impact that this interannual variability may have on ENSO evolution, most of the research performed in conjunction with interannual MJO variability seeks to understand the underlying cause of this behavior. One of the first attempts at this came from Fink and Speth (1997) who endeavored to test three (although not completely distinct) possibilities for interannual MJO variability: tropical SST, phase of ENSO, and atmospheric precipitable water. Apart from finding that the MJO propagated further east during El Niño years (see also, Gutzler, 1991; Gualdi *et al.*, 1999a; Hendon *et al.*, 1999; Kessler, 2001; Waliser *et al.*, 2001), they found no strong

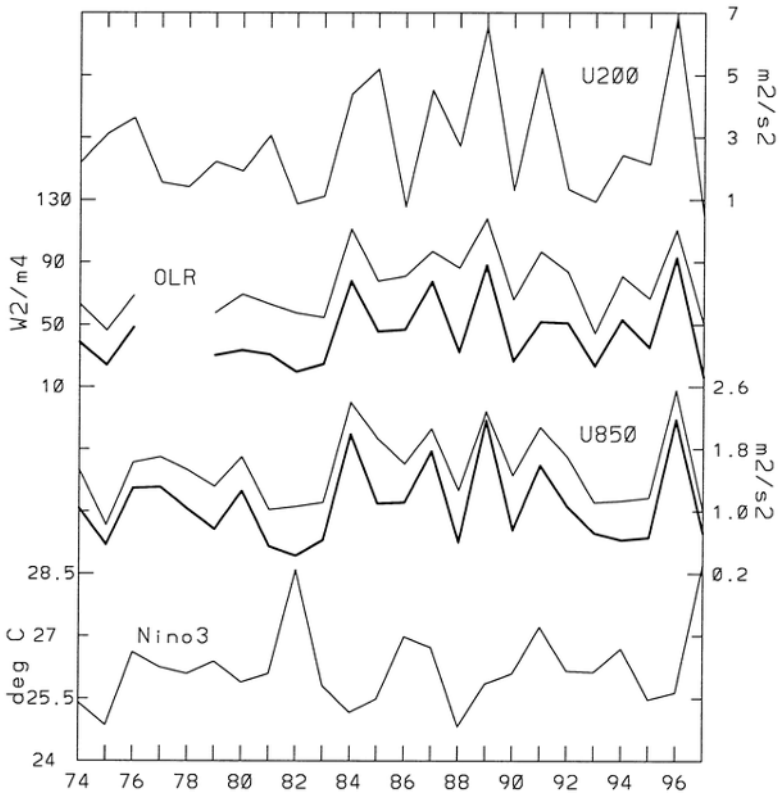

Figure 5.11. Interannual variations of MJO activity based on a number of different indices (*upper plots*) and Niño 3 SST variability (*lower plot*).
See Hendon *et al.* (1999) for details.

indicator among these three factors that could account for interannual variability of the MJO. Keep in mind that as with studies addressing the impact of the MJO on ENSO evolution, such interpretations have to be cautious about how the MJO activity is defined (e.g., Kessler, 2001; Lau, 2005). The studies by Slingo *et al.* (1999) and Hendon *et al.* (1999) each examined in some detail the observed relation between tropical interannual SST variability and MJO activity, where the latter was determined in a number of ways (e.g., OLR, low-level winds, upper level winds, principal components; Figure 5.11). The results showed that the relation was very weak, and correlations of only about −0.3 were evident between seasonal mean SST anomalies in the tropical eastern Pacific and various indices of MJO activity. Hendon *et al.*'s results indicated that most of this negative relation was associated with diminished MJO activity during the 1982–1983 and 1997–1998 El Niños. If these two periods are removed then there is virtually no correlation between the two quantities.

Given the limited observational record length and the unknowns associated with what part of the SST field is important in this regard, a number of authors have

addressed this same question via model predictability studies. The question being, given a reasonable representation of the MJO and a specification of observed SSTs, does the model's MJO exhibit any interannual predictability that could be traced to the interannual SST anomalies? Using a 4-member 45-year integration of the UK Meteorological Office (UKMO) atmospheric general circulation model (GCM; HADAM2a), Slingo *et al.* (1999) found virtually no reproducibility of the interannual variability of the MJO (i.e., only about 10% could be ascribed to external forcing). Gualdi *et al.* (1999a) used a 15-member with the ECHAM4 atmospheric GCM (AGCM) and found that with enough members (~8 or more), some evidence of year-to-year reproducibility was found (~20%). Similar results for the MJO were also found by Waliser *et al.* (2001) who used a 10-member 10-year integration with the NASA/GLA AGCM. Considering all the results above, it would appear that in general MJO activity is, at best, only weakly related to interannual SST variability, albeit the study by Chen *et al.* (2001) suggests that there might be decadal modulations to this relationship.

The above study by Waliser *et al.* (2001) also includes an examination of the same question for the boreal summer ISO. Overall, the results were analogous to those above (i.e., on average, only a very weak relation between interannual SST and ISV was found). However, the ensemble did demonstrate significantly enhanced predictability during the spring of 1982/1983. This same characteristic was found during the spring of 1997/1998 in a second 10-member ensemble that was conducted for the period September 1996–August 1998. In each of these cases, the ensemble means exhibited a decrease in ISV activity, a feature that is also echoed in the observations. Such behavior was also found in the modeling study of Krishnan and Kasture (1996). In an observational assessment, Lawrence and Webster (2001) found there to be very little relationship between ENSO and boreal summer ISO activity. While these results are suggestive of at most intermittent predictability of boreal summer ISO activity, the results of the observational analysis by Teng and Wang (2003) illustrated in Figure 5.12 indicate a much more robust relationship. These two panels illustrate the interannual variability in ISV associated with boreal summer ISV activity, distinguishing between the early summer, near-equatorial eastward propagating variability (upper) and the later summer, northern tropics, westward propagating variability (lower). In each case, there is a significant positive relationship with interannual eastern Pacific SST variability (~0.7 and ~0.6, respectively).

The contrast between the Teng and Wang (2003) results and those described above raises two questions. First, why is there such a strong seasonal dependence in the interannual connection to SST for the eastward-propagating component of ISV? Based on the various methods of analysis, and considering the discussion of Teng and Wang, the difference may lie in the degree to which the activity over the Indian Ocean is weighted into the analysis. For example, the global and empirical orthogonal function (EOF)-based measures used by the model and MJO-based studies discussed above (i.e., not the Teng and Wang study) may not be sensitive to subtle increases in ISV activity in the Indian Ocean during El Niño. Also, most AGCMs, including the NASA/GLA model used by Waliser *et al.* (1999a) exhibit

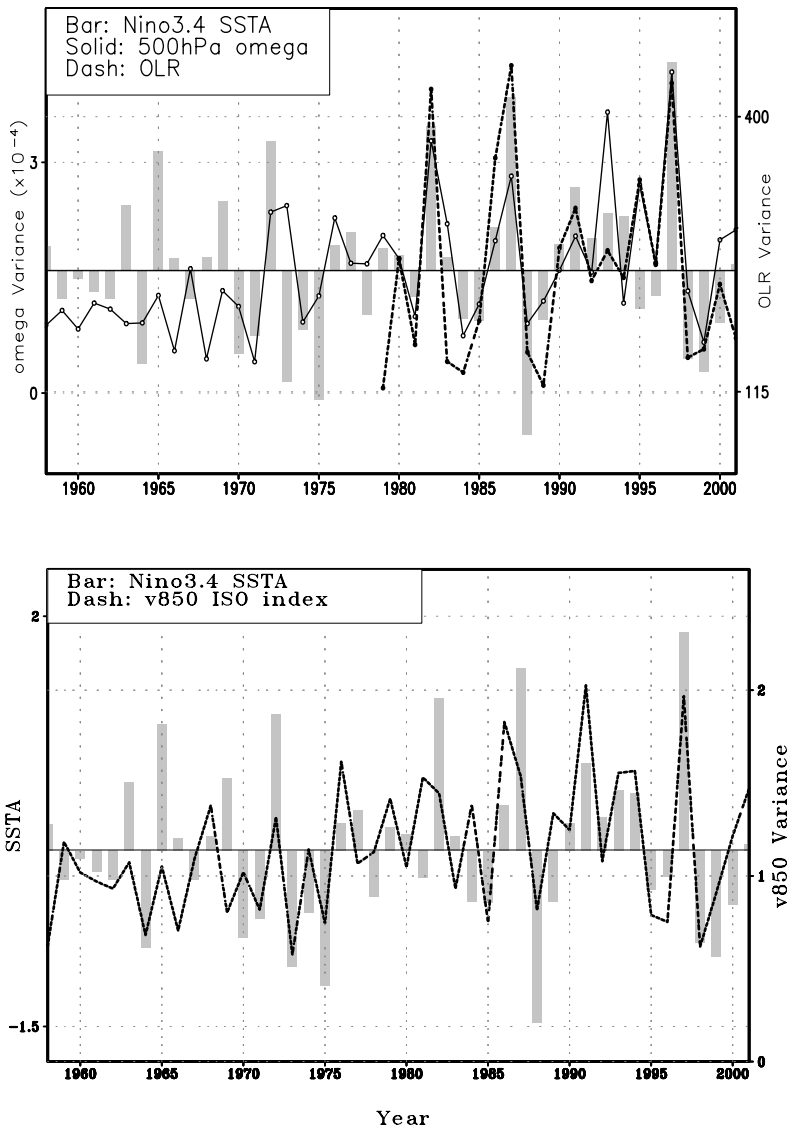

Figure 5.12. (*upper*) May–July 500-hPa vertical velocity MJO index (solid) during 1958–2001, the OLR MJO index (dash) during 1979–2001, and May–July mean Niño 3.4 SST anomaly (bar; see scale on lower plot) during 1958–2001. Vertical velocity and OLR data taken from the NCEP/NCAR Reanalysis (Kalnay *et al.*, 1996) and the OLR construction of Liebmann and Smith (1996), respectively. The MJO index is defined as the mean spectrum density for 20–50-day eastward-propagating wavenumber 1 (at 40°E–180°) anomalies averaged at 2.5°S–5°N for the vertical velocity and at 5°S–10°N for OLR. (*lower*) Similar to upper diagram, except for July–October mean Niño 3.4 SST anomaly (bar) and mean spectrum density of 10–50-day wavenumber 1–3 (at 100°E–180°) westward-propagating 850-hPa meridional wind anomaly (dash) at 5°–20°N. From Teng and Wang (2003).

relatively weak ISV activity in the Indian Ocean (Waliser *et al.*, 2003e) and thus may be incapable of reproducing the correct relationship for this part of the tropical ocean. Some evidence for the above reasoning comes from the modeling study of Krishnan and Kasture (1996). Beyond this degree of understanding, it is still yet to be fully determined how the eastward component of boreal summer ISV activity is connected to ENSO-related interannual SST variability. The second question is why does the westward propagating component exhibit a positive relation? Teng and Wang argue that this enhancement is based on the increased easterly vertical shear in association with developing El Niños. This enhanced easterly shear facilitates the emanation of the westward propagating Rossby waves which form the dynamical basis of the westward propagating variability (Wang and Xie, 1996; Xie and Wang, 1996). As yet, no model-based study has been undertaken to determine the degree to which this latter relationship can be represented in GCMs and exploited in predictions.

The second category of studies mentioned above involves understanding how the interannual variability of the monsoon may be influenced by the interannual variability of ISV, which for the most part have been directed towards boreal summer conditions (for boreal winter, see Hendon *et al.*, 1999 and Wheeler and McBride, 2005). For example, the study by Yasunari (1980) found that intraseasonal 'cloudiness fluctuations' exhibited longer periods during El Niño years. While the sample for this study was very limited, the modeling results of Krishnan and Kasture (1996) support this finding. The results of their study also suggested that El Niño conditions could influence the timescale of ISO-like oscillations in the monsoon region through the interaction with the reverse Hadley circulation (RHC) set up by the large-scale monsoon flow. The study by Teng and Wang (2003) discussed above would suggest that the character of the monsoon should be influenced via the ENSO-related sensitivity of the north-westward propagating component of the ISO. Another form of interannual modulation of the character of the monsoon arises from variations in onset dates, some of which may actually arise from the influence of the boreal summer ISO (Wu and Wang, 2000; Flatau *et al.*, 2001; Flatau *et al.*, 2003).

Another line of research in this second category of studies follows from the study of Ferranti *et al.* (1997). They studied the relationship between interannual and intraseasonal variability in a 10-member ensemble of 10-year ECMWF (European Centre for Medium-Range Weather Forecasts) climate simulations and found that the interannual and intraseasonal fluctuations share a common mode of spatial variability. That is to say that 'wet' ('dry') monsoon years would tend to have an anomalous structure along the lines of the 4th (2nd) panel of Figure 5.4. Similar results concerning the spatial structure of the dominant interannual and intraseasonal modes were found in an observational analyses of Annamalai *et al.* (1999) and Sperber *et al.* (2000). In the latter study, they showed that the probability distribution function (PDF) of the principal component time series of the dominant mode of subseasonal variability undergoes a shift in its mean, not its (Gaussian) form, between weak and strong monsoon years. Additional analysis indicated that these shifts were primarily due to changes in the basic state. For example,

Annamalai *et al.* (1999) found that El Niño tended to predispose the PDFs of the principal components of the leading intraseasonal modes toward more break conditions (see, e.g., the 2nd panel of Figure 5.4). Along similar lines, Molteni *et al.* (2003) examined an ensemble of seasonal hindcasts and found that the 2-D PDF of the principal components of the two leading intraseasonal modes changed from a unimodal distribution during El Niño to a bimodal distribution during La Niña. Lawrence and Webster (2001) examined the relation between interannual monsoon variability (i.e., seasonal mean OLR anomalies) and the amount of intraseasonal variability within the season and found that ISO activity exhibits a strong inverse relationship with the seasonal mean Indian summer monsoon strength. In an analysis of both long-record reanalysis and OLR data, Goswami and Mohan (2001) also found the common mode of interannual variability and argued that wet (dry) monsoon years were simply associated with a greater frequency of occurrence of the active (break) phase of the ISO.

While there are a number of common links in the studies above which suggest that monsoon ISO variability might undergo regime changes related to ENSO, there is still a need to sort out more clearly the effects from ENSO, how this may change over the course of the monsoon season, and if there is a decadal modulation of this influence? In addition, there still seems to be a debate regarding whether or not the level and type of boreal summer ISO activity influences the seasonal mean monsoon? If it does, and it turns out that the ISO activity is largely insensitive to interannual SST variability (e.g., ENSO), then this makes the problem of seasonal prediction of the monsoon particularly difficult.

5.4.2 Rectification onto low-frequency variability

The material at the end of the previous subsection highlights the fact that the nature of the intraseasonal variability over a given period (e.g., season) can produce variability on a longer timescale. For example, the results of Lawrence and Webster (2001) discussed above indicates that more (less) ISO activity is associated with a weaker (stronger) seasonal monsoon rainfall. While it is far from clear what aspect of the variability presupposes what, it is clear that ISV involves significant and important timescale interactions. A similar line of research considers this question more directly (i.e., how does the presence of ISV alter the basic state of the atmosphere and/or ocean systems?). The first explicit study along these lines was by Kessler and Kleeman (2000) who considered the questions of how the MJO might modulate the mean state of the ocean, as well as how it may influence the development and evolution of El Niño? As indicated above, the latter of these lies outside the scope of this chapter and is best addressed by the other reviews cited. Briefly, the former part of their examination involved comparing the differences in the response of a tropical Pacific ocean with annual cycle forcing and annual cycle forcing plus an analytical representation of idealized MJO forcing. Their results showed that the low-frequency (e.g., seasonal mean timescale) ocean response to the MJO in the equatorial western Pacific consisted of a cooling ($\sim 0.4^{\circ}$C) and eastward current anomaly ($\sim 0.2\,\mathrm{m\,s^{-1}}$). Such values are considerable in the context of coupled

climate modeling and climate change scenarios, particularly given that at least in some cases there seems to be an influence of SST on the MJO itself (see discussion above and in Section 5.5).

The study by Waliser *et al.* (2003b) examined the same rectification issue with the same model and considered the Indian Ocean as well. In addition, in their study the MJO forcing was based on a composite construction from observations. For the boreal winter analysis, and thus the MJO, the low-frequency ocean response consisted of a much weaker cooling ($\sim$0.1°C) in the equatorial western Pacific (and Indian) Ocean region, a relatively larger warming in the Maritime Continent region ($\sim$0.3°C), a fair amount of mixed layer depth (MLD) shallowing ($\sim$5 m) in most of the above regions, and a westward equatorial Pacific Ocean current anomaly ($\sim$0.1 m s^{-1}). The reasons for the differences between these results and those of Kessler and Kleeman (2000) are too numerous to elaborate on here but include the differences in MJO forcing, model vertical resolution, and the manner in which wind 'gustiness' was handled. The main points to emphasize here are that there is evidence for a low-frequency effect onto the ocean from ISV but yet too few studies to make any sort of robust determination – even in the sign of the effect.

For their boreal summer study, Waliser *et al.* (2004) showed that the imposed ISO forcing and associated ocean response exhibit a low-frequency rectification, namely a mean SST warming ($\sim$0.1°C) and MLD shoaling ($\sim$7 m) over much of the northern Indian and north-western tropical Pacific Oceans. The rectified SST signal was found to be mostly associated with a rectified signal in the short-wave forcing, although the MLD shoaling resulted mostly from non-linear mixed layer processes. The rectified signal in the short-wave forcing comes about through the large-scale organization of the ISO/MJO, namely that the convective/cloudiness anomaly organizes itself over smaller spatial scales than the corresponding subsidence region – a feature common to convection at all scales. The net effect is that over the life cycle of the MJO/ISO there is slightly more positive surface solar heating than surface cooling. This feature was also discussed in the context of rainfall and water vapor in the study of Myers and Waliser (2003). A related examination by Shinoda and Hendon (2002) regarding the rectified enhancement of wind speed and latent heat flux by the MJO found both quantities enhanced ($\sim$1 m s^{-1} and 20 W m^{-2}) over the western Pacific when averaged over the life cycle of a typical MJO. The most recent study involving rectification is that of Han *et al.* (2004) who used a model framework to show that imposed intraseasonal wind variability acts to weaken the equatorial seasonal surface currents, in part due to the asymmetric response of the ocean mixed layer to wind direction and vertical processes. Taken together, the above studies indicate that the potential for rectifying ISV onto longer timescales exists. While more research is needed in this area, there is presently enough evidence to suggest that these issues be taken into account when considering a (coupled) model's representation of climate in conjunction with its ability to properly represent the ISV.

While the discussion in this section has only been able to provide a brief review of the low-frequency variability associated with ISV (see Chapter 7 for discussion of decadal variability), it illustrates the very complex interplay between

the intraseasonal and longer timescales that contain both upscale and downscale interactions. Moreover, the discussion makes it painfully obvious that very few firm hypotheses or answers exist regarding mechanisms, and in some cases there is still not a confident determination of the basic nature of the relationships – even in a statistical sense. This all serves to illustrate that this area of ISV research on one hand is largely in its infancy and at this point is probably most hindered by a lack of quality, long-term data and/or models with which to further address the problem rather than a lack of interest or merit in the problem.

5.5 THEORY AND PHYSICAL PROCESSES

While the theory for many tropical wave motions (Matsuno, 1966) tended to precede their observation and characterization, the opposite is the case for the MJO/ISO (Madden and Julian, 2005). Since the discovery of this phenomenon, there has been ample opportunity and data sets to characterize many of its basic features. However, the articulation of a succinct and somewhat well agreed upon theory has remained a challenge. Most notably this has been due to the fact that on the one hand the MJO/ISO is a planetary-scale phenomenon yet it is apparent that cumulus convection, and its organization on a wide range of time and space scales (Nakazawa, 1988; Lau *et al.*, 1991), is an inherent and vital component. In addition, there appears to be non-trivial interactions with the mean state circulation, the surface conditions – including coupling to the ocean, clouds, radiation, and possibly even mid-latitude variability. Distilling these processes and features into something simple enough to be coined a 'theory', yet retaining enough complexity to provide for adequate realism when judged against observations, makes this task particularly difficult. This section reviews the physical processes that are thought to play a key role in producing the MJO/ISO and the theories that have been put forward to try and succinctly capture the physical essence of the phenomenon. As with much of the material above, the theoretical developments pertaining to the boreal summertime ISO have largely followed from research initially put forth to describe the MJO. Thus, this section first discusses these topics with regard to the MJO, with an effort to limit the discussion to only the most essential aspects. Then, the final subsection discusses the same set of issues as they pertain to the boreal summer ISO. For a more thorough review of this subject, the reader is referred to Wang (2005).

5.5.1 Atmospheric dynamics

As the MJO was most readily observed in the atmosphere in terms of wind and cloud fluctuations, the early theories focused on instability mechanisms dealing primarily with the atmosphere alone. The first notable inroad for providing some theoretical basis for the MJO involved a form of conditional instability of the second kind (CISK). The concept of CISK was developed to explain the intensification of tropical depressions into hurricanes as well as the maintenance of the latter (Charney and Eliassen, 1964; Ooyama, 1964). The concept was developed further to examine possible interactions between cumulus convection and the large-scale

divergence field of tropical waves (Yamasaki, 1969; Hayashi, 1970; Lindzen, 1974a,b). In these studies, low-level convergent (divergent) areas of equatorial wave motions were tied to atmospheric heating (cooling) to examine the influence on instability growth and propagation speed. The most notable shortcomings of the earliest contributions in this area involved a tendency to amplify short rather than planetary-scale waves and to have phase speeds for the excited waves propagating too fast.

There have been a significant number of variations on the wave–CISK theme to remedy these shortcomings. For example, changing from a linear heating formulation to a non-linear one (e.g., positive heating for upward motion but no cooling for downward motion) does allow for planetary-scale descending regions but at the cost of having the convective region reduced to the smallest scale, either grid-scale in a numeric framework (Lim *et al.*, 1990) or infinitesimal in an analytic framework (Dunkerton and Crum, 1991; Wang and Xue, 1992). One line of research to reduce the phase speed of conventional wave–CISK modes involves varying the specification of the vertical heating profile or the inclusion of the first two gravest vertical modes (Lau and Peng, 1987; Chang and Lim, 1988; Mapes, 2000). There has yet to be resolution on this issue as Takahashi (1987) and Sui and Lau (1989) found that heating maximized in the lower troposphere tended to favor MJO-like modes while Cho and Pendlebury (1997) found that heating, maximized in the upper troposphere, was better. Additional work in this area has shown sensitivity to the parameterization of the convective heating (Neelin and Yu, 1994) and the inclusion of non-linear advection (Hendon, 1988).

Another significant variation on the wave–CISK theme provides for coupling the free atmosphere to a frictional boundary layer (Wang, 1988a; Salby *et al.*, 1994). Inclusion of boundary layer friction results in an apparent 'coupling' between moist Kelvin and Rossby modes (Wang and Rui, 1990b). One of the fundamental features of this paradigm, often referred to as 'frictional wave–CISK', is that to the east of the convective heating the low-level winds associated with the Kelvin wave component turn equatorward in response to the friction and produce a region of low-level moisture convergence. This process favors both eastward propagation of the convective system and thus the entire planetary structure but also acts as an important source of energy for growth/maintenance. The inclusion of the Rossby mode under this framework also favors the development of the planetary scale, slows down the eastward propagation to values more consistent with observations, and plays an important role in dissipating energy that would otherwise cause the pure wave–CISK Kelvin wave instability to grow unrealistically fast. It should be noted that Moskowitz and Bretherton (2000) showed that the qualitative wave destabilization effects from friction appear to be insensitive to the convective parameterization employed which suggests that the theoretical basis for frictional wave–CISK is not necessarily tied to subjective choices in its implementation. On the other hand, they also argue that the values of surface drag used in the earlier study by Wang and Rui (1990b) are unrealistically large which overemphasizes the contribution of frictional wave–CISK to the mechanism of MJO instability (see counter argument in Wang, 2005).

As illustrated in the MJO life cycle maps constructed by Hendon and Salby (1994), there is strong observational evidence that the dynamical structure of the MJO does exhibit both Kelvin and Rossby wave components. An analogous figure from their study for the low-level wind structure indicates easterly zonal wind anomalies to the east of the convection, consistent with Kelvin wave dynamics, but which have a convergent meridional component consistent with the impacts of friction. A number of additional studies have shown evidence that supports the notion of low-level frictional moisture convergence to the east of the convection which appears at least consistent with frictional wave–CISK (e.g., Jones and Weare, 1996; Maloney and Hartmann, 1998; Matthews, 2000). In addition, there have been a number of diagnostic studies of model simulations of the MJO that have illustrated the frictional wave–CISK mechanism at work within the model generated MJOs (e.g., Lau and Lau, 1986; Lau *et al.*, 1988b; Sperber *et al.*, 1997; Waliser *et al.*, 1999a; Lee *et al.*, 2003).

In contrast to the wave–CISK mechanism(s), which operates on the principal that latent heat release from convection is an important source of energy for the instability, the 'evaporation–wind feedback' theory ((Emanuel, 1987; Neelin *et al.*, 1987), often later referred to as wind-induced surface heat exchange (WISHE; Yano and Emanuel, 1991)) claims that diabatic heating due to cumulus convection is nearly compensated by adiabatic cooling. Further, it is assumed that a region of anomalous convection forces low-level easterly winds to the east and low-level westerly winds to the west of the convective region. If large-scale convection is present in a region of mean easterly winds, the strength of the wind speed anomalies (and likely the evaporation anomalies) is increased to the east and decreased to the west of the convective region. The positive anomalies of surface latent heat flux to the east of the convection increase the low-level moist static energy, which leads the wave vertical velocity and induces unstable eastward propagating modes that exhibit some resemblance to the MJO.

The evaporation–wind feedback theory has been criticized based on the fact that over a large portion of the eastern hemisphere where the MJO is most prevalent, the climatological winds are extremely weak or even westerly (Wang, 1988). Neelin (1988) and Emanuel (1988) argued that given the large zonal scale of the MJO, the requirement for mean easterlies to the east of the convection typically holds in most cases of convection occurring in the eastern Indian Ocean and western Pacific. While the MJO does have a planetary scale at upper levels, particularly in regards to wind, the wind's interaction with convection in the eastern hemisphere significantly reduces its zonal length scales of variability, especially near the surface. Thus, while it is understood that the above mechanism doesn't fit with observations in the western/central Indian Ocean, it may not be very plausible to cite in regards to the eastern Indian and western Pacific either. A related difficulty facing the evaporation–wind feedback theory comes from a number of studies that document the observed relation between deep convection and evaporation associated with the MJO. These studies have shown that evaporation anomalies are typically higher to the west, rather than to the east, of the convection anomaly (Jones and Weare, 1996; Lin and Johnson, 1996b; Lau and Sui, 1997; Jones *et al.*, 1998; Shinoda *et al.*, 1999;

Woolnough *et al.*, 2000), which is at odds with one of the central premises of the evaporation–wind feedback theory. This behavior has also been observed in some of the more successful modeling simulations of the MJO (Sperber *et al.*, 1997; Waliser *et al.*, 1999a).

A couple of additional points that have relevance to the evaporation–wind feedback theory and the discussion above can be drawn from the following modeling studies. First, it is worth noting that recent analysis suggests that in order for a GCM to exhibit a robust eastward propagating MJO, it is necessary that the model produces a good simulation of the equatorial westerlies that extend from the Indian Ocean well into the western Pacific (Waliser *et al.*, 2003a; Sperber, 2004). Second, Kirtman and Vernekar (1993) examined a simplified model that contains both the wave–CISK and evaporation–wind feedback mechanisms and found that the model wave speeds were found to better match the observed speeds over a wider range of parameter values for the combined mechanism than for evaporation–wind feedback acting alone. Lin *et al.* (2000) examined the relative roles of evaporation–wind feedback and mid-latitude forcing of the MJO in an idealized GCM and found that evaporation–wind feedback alone was not a sufficient mechanism to produce MJO variability of adequate amplitude and that the forcing from mid-latitudes was, at least in that model, an important source of MJO forcing (see also Hsu *et al.*, 1990; Slingo, 1998). Finally, based on sensitivity experiments from an AGCM coupled to a slab mixed layer with different depths (e.g., 2–50 m), Maloney and Sobel (2004) showed that the model exhibits realistic amplitudes of intraseasonal convection only when SST variations, and thus in turn its effects on evaporation–wind feedback, are properly phased relative to the intraseasonal convection anomalies.

Apart from the MJO instability/maintenance mechanisms discussed above, a number of studies have suggested mechanisms that are driven by local feedbacks. For example, both Hu and Randall (1994, 1995) and Raymond (2001) argue for the role of radiative–convective feedbacks. In the latter case, clouds associated with the convective event trap long-wave radiant energy and lead to additional tropospheric heating that helps to destabilize the event. While past studies in this area have generally been based on GCM work and have not lead to any conclusive/comprehensive results (Slingo and Madden, 1991; Mehta and Smith, 1997; Lee *et al.*, 2003), the recent diagnostic study by Lin and Mapes (2004) has estimated that atmospheric integrated radiative heating may augment the condensational heating by as much as 10–15%. In another variation, Blade and Hartman (1993) argued that the timescale associated with the MJO derives from the time for the large-scale convection event to evolve through its life cycle (and thus 'discharge' the excess moist static energy) plus the time it takes the atmosphere to moisten again (and thus 'recharge'). They referred to this theory as the 'discharge–recharge' hypothesis. A number of additional studies have also suggested the importance of water vapor feedback in the regards to the MJO (Goswami and Mathew, 1994; Woolnough *et al.*, 2000; Kemball-Cook and Wang, 2001). The relevance of the above types of mechanisms cannot be ruled out at this stage. Even though the MJO/ISO is not consistent with a stationary oscillation (Zhang and Hendon, 1997) that might ensue when considering only local feedbacks,

it is quite possible that the above sorts of mechanisms play complimentary roles to those that are based on a wave-like infrastructure (Sobel and Gildor, 2003). For example, it could be that these local feedback mechanisms do play a role in establishing the instability and in some sense setting the timescale, and the wave activity simply propagates the signal, and in some cases these two processes can constructively (destructively) interact (e.g., via circumnavigation) to produce very robust or very weak MJO/ISO seasons.

Within the recent review of MJO theory by Wang (2005) is an attempt to provide a comprehensive or universal view of MJO/ISO theory (see his Figure 10.1) taking into account the most essential processes and feedbacks. Embedded within this discussion is a distillation of a simplified theoretical model of the MJO as well as the ISO. The fundamental mode of instability for the MJO is referred to as the 'frictional CID'. In regards to terminology, this is a combination of 'frictional wave–CISK' and 'convective interaction with dynamics' (after Neelin and Yu, 1994). The basics of the instability derive from low-frequency equatorial waves, convective latent heating, boundary layer dynamics (i.e., friction), and some accounting for the spatial distribution of atmospheric moisture. Generally speaking, this instability and the equations it derives from are the same as those associated with 'frictional wave–CISK' discussed above. However, given the instability occurs in a dynamic regime stable to wave–CISK, that the overall processes involved are consistent with CID, and that the frictional boundary layer component is so essential, the author deemed 'frictional CID' as the most appropriate terminology. For a more complete description of the equations and a quantitative analysis of the instability, the reader is referred to Wang (2005).

5.5.2 Air–sea interaction

Most of the early observational research regarding the MJO/ISO focused on upper level winds and satellite data such as the OLR. This is due at least in part to a dearth of near-surface observations with adequate time and spatial resolution to sample the MJO/ISO. However, as it became clear that the MJO was a recurrent and pronounced signature in the tropical climate, attention started to turn toward near-surface conditions and the interaction of the MJO with the ocean. This began with the study by Krishnamurti *et al.* (1988) who detected sizable intraseasonal variations in a number of near-surface meteorological quantities that directly influence the turbulent heat exchange as well as in SST. Little more was done in this area until the advent of a number of new data sources that included TOGA/TAO, TOGA COARE, atmospheric reanalysis products, and remotely sensed (near-) surface measurements via satellite. From this point, a wealth of studies documented the relationships between the MJO, air–sea heat, momentum and mass fluxes, and SST (e.g., Krishnamurti *et al.*, 1988; Jones and Weare, 1996; Lin and Johnson, 1996b; Waliser, 1996; Weller and Anderson, 1996; Zhang, 1996; Hendon and Glick, 1997; Lau and Sui, 1997; Jones *et al.*, 1998; Shinoda *et al.*, 1998; Woolnough *et al.*, 2000; Shinoda and Hendon, 2001; Waliser *et al.*, 2003b).

From the studies listed above, it has become abundantly clear that, at a

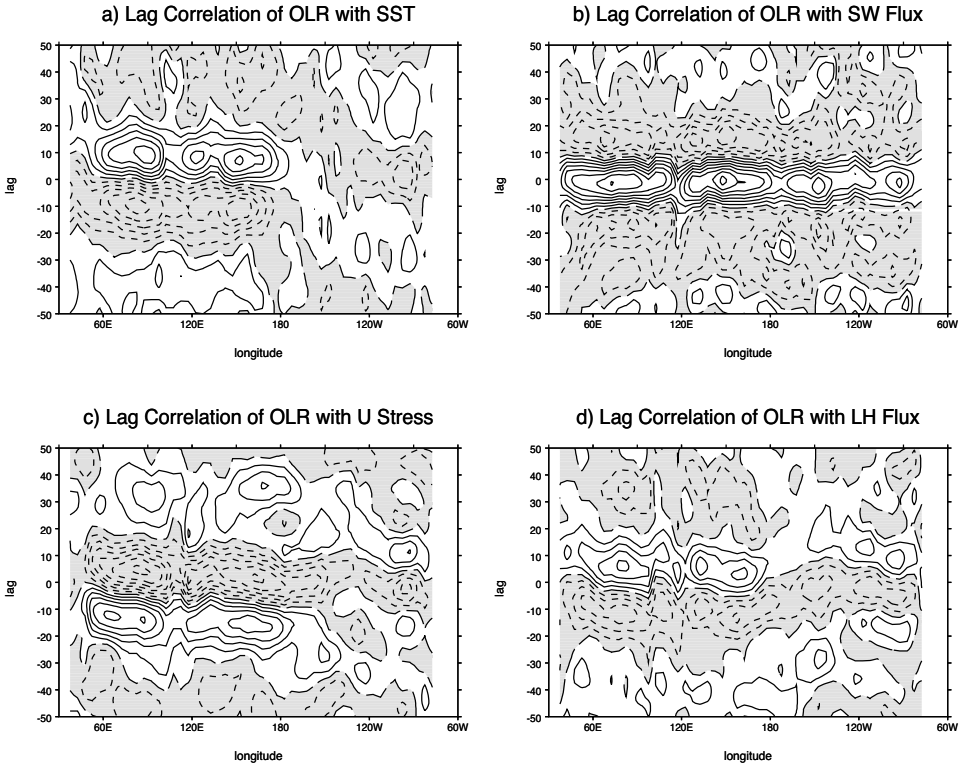

Figure 5.13. Lag correlations between OLR (convection) and surface fields (SST, short-wave flux (SWF), latent heat flux (LHF), zonal wind stress (UST)). Negative lags indicate that the convection lags the surface field; positive lags indicate that the convection leads the surface fields. The sign convention is such that positive correlations indicate that enhanced convection (a negative OLR anomaly) is correlated with a negative SST anomaly, reduced SWF at the surface, a negative LHF anomaly at the surface (enhanced evaporation), or an easterly wind stress anomaly. Negative correlations are shaded; contour interval is 0.1, with negative contours dotted; and the zero contour is dashed. Correlation coefficients above 0.103 at zero lag and 0.116 at 50-day lag are significant at the 95% level based on $N/10$ degrees of freedom, the minimum number of points required to resolve variations with the largest retained frequency.
From Woolnough *et al.* (2000).

minimum, the MJO strongly modulates air–sea fluxes and SST on the intraseasonal timescale. For example, Figure 5.13, taken from Woolnough *et al.* (2000), shows a very robust relationship between convection and each of the following: SST, wind stress, and surface latent and short-wave flux, over much of the eastern hemisphere tropical oceans. The plots show that positive anomalies in convection lead positive anomalies in wind stress and latent heat flux and lag positive anomalies in SST and short-wave flux. Put another way, to the east of the convection, surface easterly anomalies within a westward mean state and subsidence driven clear skies imply

SST-warming flux anomalies for both evaporation and short-wave fluxes. As the convection passes over the anomalously warm water the cloud-induced negative short-wave anomalies and enhanced surface westerly anomalies imply SST-cooling flux anomalies. To gain an appreciation of the magnitude of the variations, Figure 5.14, taken from Shinoda *et al.* (1998), shows the typical variations of these quantities during the TOGA COARE period. From this and the other studies above, it is well known that MJO-related surface latent and short-wave flux variations can easily exceed $\pm 50\,\mathrm{Wm}^{-2}$, SST variations often exceed 0.5°C, and zonal wind (stress) variations can exceed $5\,\mathrm{m\,s}^{-1}$ ($0.4\,\mathrm{N\,m}^{-2}$). Along with these intraseasonal changes, there is even an indication that the MJO strongly modulates the character and size of the diurnal variations of these quantities (Weller and Anderson, 1996; Shinoda and Hendon, 1998).

Given the observational developments described above, the reigning interest and understanding of the close ocean–atmosphere coupling that exists in the tropics (e.g., TOGA COARE, ENSO), and the recurrent shortcomings in AGCM representations of the MJO, the community began to hypothesize a role for air–sea coupling in the manifestation of the MJO (e.g., Kawamura, 1988, 1991; Li and Wang, 1994; Jones and Weare, 1996; Waliser, 1996; Sperber *et al.*, 1997). In particular, the question was raised how do the intraseasonal variations in SST and surface heat fluxes – which to first order appear driven by the MJO – feedback and influence the MJO itself? Given the nature of this problem involves testing a feedback, the most suitable, albeit limiting, framework for its examination is in a modeling context. The first studies having some relevance to this problem were by Lau and Shen (1988) and Hirst and Lau (1990). Stemming from an intense period of theoretical ENSO research, they developed theoretical coupled ocean–atmosphere models to explore the instability of high-frequency coupled equatorial disturbances. The ocean coupling in these models was limited to a simplified interactive SST based only on thermocline dynamics. While the results of these studies showed a particular regime of high-frequency coupled instabilities, it came at the expense of unrealistic treatments of dissipation and/or neglect of the Coriolis force. The idealized form of the coupling in these studies severely limited the thermodynamic influence of the ocean mixed layer, an interaction that would be expected to be important given the nature of the Indo–Pacific warm pool and observational studies mentioned above.

Wang and Xie (1998) extended these studies (or rather the frictional wave–CISK studies discussed above) by adding a fairly sophisticated mixed layer feedback that takes into account MJO-forced variations in surface heat and ocean mixed layer entrainment fluxes. Their model indicated that the feedback from wind-driven entrainment/evaporation, and to a lesser extent by the clouds/radiation, were largely responsible for slowing and destabilizing what would otherwise be a neutral moist Kelvin wave in the uncoupled model. In their analysis, slow disturbances with low wavenumbers were preferentially destabilized, since they would be the most effective at modifying and interacting with SST. The results of their study provide a theoretical basis for the suggestion that SST variations provide an important feedback on the MJO, and in particular, that ocean mixed layer physics are an important element in this feedback.

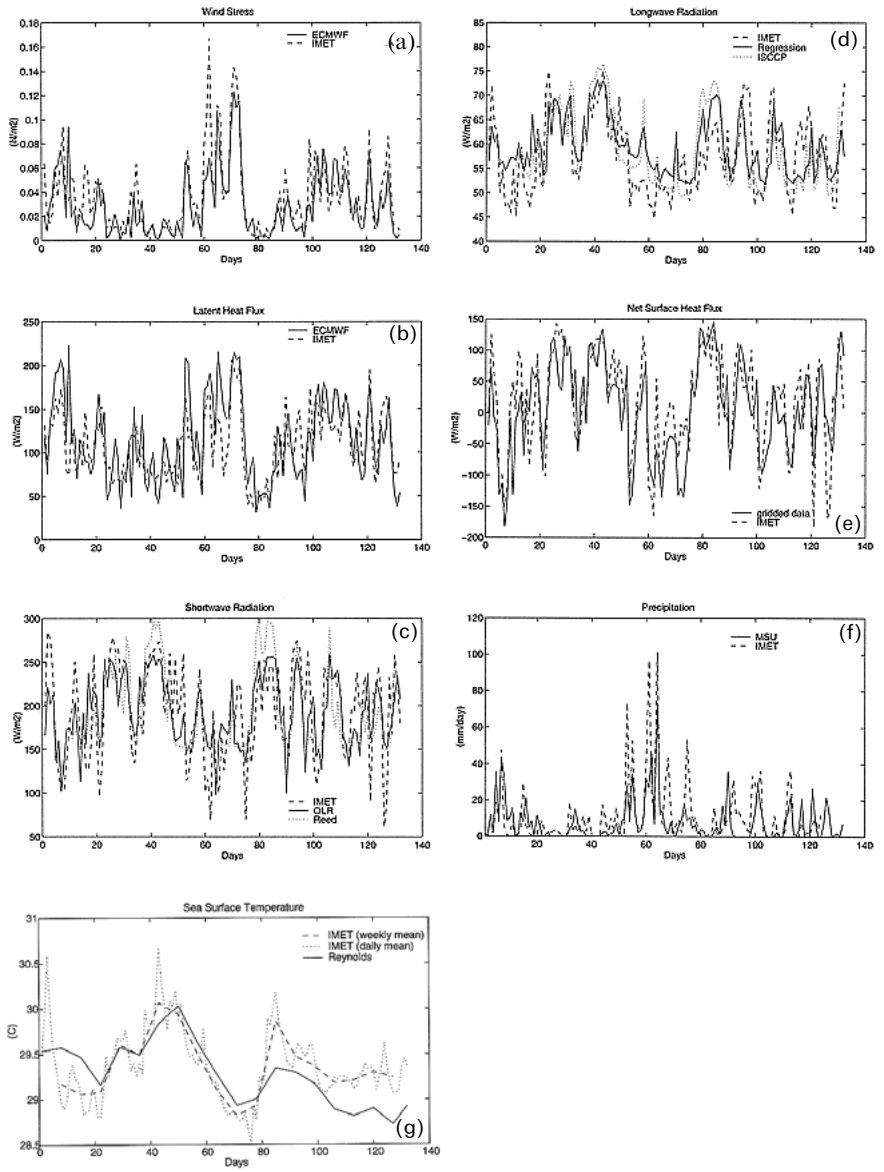

Figure 5.14. Time series of (a) wind stress, (b) latent heat flux, (c) short-wave radiation, (d) long-wave radiation, (e) net surface heat flux, (f) precipitation, and (g) SST for TOGA COARE on 22 October 1992 through to 2 March 1993. Dashed lines in (a)–(f) indicate daily mean flux estimates from the IMET mooring observations sited at 1°45′S, 156°E. The dashed line in (g) indicates the weekly mean SST from the IMET mooring observations. Thick lines indicate estimates from gridded data centered at 2.5°S, 155°E. The dotted line in (c) indicates the short-wave flux estimated from the formula by bulk formula. The dotted line in (d) indicates net long-wave flux estimated from bulk formula using ISCCP total cloudiness. The dotted line in (g) indicates the daily mean SST from the IMET mooring observations. From Shinoda *et al.* (1998).

Over the past few years a number of numerical studies have addressed the role of SST coupling and the MJO. For example, Flatau *et al.* (1997) employed a simplified GCM (e.g., Lau and Peng, 1987) coupled to an empirically derived slab ocean mixed layer feedback. They found that the addition of the SST feedback produced a stronger and more organized form of intraseasonal variability. They proposed that the zonal gradients in SST anomalies near the region of convection can create zonal gradients in surface moist static energy which favors the formation of convection in the wave convergent region and thus helps to amplify the power of the oscillation. They termed the mechanism Air–sea Convective Intraseasonal Interaction (ASCII). Unfortunately, the simplicity of the GCM used in their study prevented any conclusive analysis (e.g., on the surface heat flux or planetary boundary layer (PBL) moisture budget) that would directly support this hypothesis.

Waliser *et al.* (1999a) found that when their AGCM was coupled to a (50 m) slab ocean mixed layer the interactive SSTs had modest but important impacts in the simulation of the MJO, with the characteristics of the coupled model's MJO being closer to those observed. These impacts included (1) the increased variability associated with the MJO, (2) the tendency for the timescales of modeled intraseasonal variability to be around those found in the observations, (3) a reduced eastward phase speed in the eastern hemisphere and (4) an increased seasonal signature in the MJO with relatively more events occurring in the December–May period. They attributed the better simulation to the feedback with the SSTs. They suggested that the enhanced SSTs, forced by decreased latent heating and increased short-wave flux to the east of the positive convective anomalies tended to reinforce the meridional convergence associated with the frictional wave–CISK mechanism working within the AGCM. This meridional convergence increased the moist static energy that acts to destabilize the model's MJO. It is interesting to note that in both the above numerical studies, some element of the MJO did exist without coupling – as is often the case with AGCMs (Slingo *et al.*, 1996; see Section 5.6), yet in Wang and Xie's theoretical study, the instability only exists upon coupling. This raises an important question regarding whether the MJO is inherently a coupled phenomena or whether interactive SST simply provides a modulating feedback (see Waliser *et al.* 1999a for further discussion).

In another GCM study, Hendon (2000) explored the impact of air–sea coupling on the dynamics of the MJO in a GCM coupled to a 1-D ocean mixed layer model. In that study, Hendon found that coupling had no significant influence on the simulation of the MJO. However, analysis of the model results showed that the simulated MJO-induced latent heat flux anomalies were relatively incoherent and did not exhibit the proper (i.e., observed) phase relationship relative to the convection, in part due to the model's basic state (see evaporation–wind feedback discussion above). Thus, the latent heat flux anomalies did not constructively interact with the MJO-induced short-wave anomalies to produce the needed/observed systematic changes in the anomalous SST that in turn could influence the MJO. Thus, to some degree, this study's findings highlight the necessity for a proper representation of the basic state when simulating the MJO rather than have implications on the SST–MJO coupling question directly (see also Gualdi *et al.*, 1999b). Additional important work

in this area includes the studies by Inness and Slingo (2003), Inness *et al*. (2003), and Sperber (2004) that emphasize the proper simulation of the basic state in terms having low-level westerly zonal winds present in regions where eastward propagation is observed/expected (e.g., Indian and western Pacific Ocean).

Wu *et al*. (2002) analyzed a particularly strong MJO event within observations and from 10-member ensemble simulations with 10 different AGCMs forced with the same observed (1996–1998) weekly SSTs but with different initial atmospheric conditions. One of the main findings in that analysis relevant to the present discussion is that while the observed convection anomalies were in quadrature with, and lagging, the associated intraseasonal anomaly in SST, the simulated MJO convection events were nearly in phase with the SST anomaly. Based on the results of the studies mentioned above, the observed relationship is understood to come about – to first order – via MJO-driven heat flux variations imparting an intraseasonal signal on SST. However, given the specified SST framework in the simulations, the modeled relationship is more accurately depicted as a 'forced' signal whereby the MJO event is responding to the SST variations in the boundary conditions. Additional support for this finding comes from the modeling study of Zheng *et al*. (2004) who compared the simulation of the MJO between a coupled GCM (CGCM) simulation and the corresponding AGCM simulation that used the SSTs from the CGCM simulation. In the coupled case, the model convection lags the SST anomalies by about 1/4 cycle (consistent with observations), while for the specified SST case, the convection and SST are nearly in phase. These results help to emphasize the importance of including air–sea coupling in the context of numerical simulations and predictions.

Additional studies supporting the notion that interactive SSTs are important to the character of the MJO include Sobel and Gildor (2003), Watterson (2002), and Maloney and Sobel (2004). These studies emphasize the sensitivity of the SST feedback to the depth of the ocean mixed layer, with the implication that the depth has to be shallow enough to provide sufficient sensitivity to the intraseasonal timescale and associated size of surface fluxes (e.g., Figure 5.14) and yet deep enough to provide a sufficient time lag between SST anomaly development and the passage of the MJO convection – considered together these imply that a mixed layer depth induces the greatest feedback to the MJO when it is O (10 m). Finally, the study by Maloney and Kiehl (2002) illustrate analogous feedbacks between SST and MJO-like variability in the eastern Pacific Ocean. Taken together, the studies highlighted in this subsection strongly suggest that a proper and complete physical description of the MJO has to take into account its interaction with the near-surface ocean, namely the SST. For a more thorough review of this area, the reader is referred to Hendon (2005).

5.5.3 Boreal summer ISO

The above two subsections provide pertinent background information on the theoretical developments associated with the MJO. While there has yet to be widespread acceptance of a single theory for the MJO, it is becoming increasingly clear at least what the main physical elements are that need to be considered. As discussed

previously, the ISO and MJO could be considered essentially the same phenomena modified by the annually changing background state. For the case of the MJO, this tends to simplify the issue somewhat since during the period it is most strongly exhibited; the warm SSTs and large-scale circulation are more symmetrically aligned with the equator. This results in a background state that has a more straightforward zonal structure and a lower boundary made up almost entirely of ocean. However, for the case of the ISO, all the same issues relevant to the MJO need to be considered but in addition it is necessary to deal with the asymmetric and off-equatorial circulations prevalent around south-east Asia in boreal summer and possibly consider a larger role for land surface interactions. In addition, the ISO's influence on, and from, the oceans and seas surrounding south-east Asia is also more complex than for the MJO, which interacts more directly with the more uniform, basin-scale oceanography of the equatorial Pacific and Indian Ocean (e.g., Waliser *et al*., 2003b, 2004).

Taking the above discussion into account, it is not surprising that theoretical and air–sea interaction studies for the boreal summer ISO analogous to those described above for the MJO are considerably fewer. However, in recent years there has been significantly more research in these areas as they pertain to the boreal summer ISO. For example, Vecchi and Harrison (2002), Sengupta *et al*. (2001), Sengupta and Ravichandran (2001), and Kemball-Cook and Wang (2001) all document similar relations between convection, surface heat fluxes, and SST as described above for the MJO – the principal difference being that the large-scale propagation includes a northerly component in addition to the eastward component (see Figure 5.4). Figure 5.15, taken from Sengupta *et al*. (2001), succinctly illustrates the fact that ahead of the northward propagating convection are clear skies, calm winds, and warming SSTs, and that upon arrival of the convection comes cloudy skies, high winds, and cooling SST. Additional evidence suggests the importance of the ocean–atmosphere coupling implied by this relationship to understand and properly model the ISO. For example, similar to the study by Wu *et al*. (2002) discussed above, the studies by Fu and Wang (2004) and Zheng *et al*. (2004) both illustrate that it is not just the intraseasonal oscillations in SST that are important but rather the inclusion of actual interactive SST coupling. The contour plots in Figure 5.16, taken from Fu and Wang, compare the spectral power in the northward propagating ISO components from a CGCM, the corresponding AGCM where the SSTs were specified from the CGCM simulation, and from observations. For this model, it is clear that the coupling has a profound and positive impact on the modeled ISO. The line plot in Figure 5.16, taken from Zheng *et al*., shows that the observed (quadrature) phase relationship between convection and SST is properly represented in their CGCM. However, the relationship becomes incorrectly represented in the corresponding AGCM simulations that use specified SSTs taken from the CGCM simulations. Nearly identical results regarding this aspect of the ISO phase relationship were also found by Fu and Wang. The results from studies such as these indicate that interactive SSTs, namely via mixed layer physics, are a crucial part of the physical makeup of the ISO and, as with the MJO, will need to be accounted for in any comprehensive theory for the ISO.

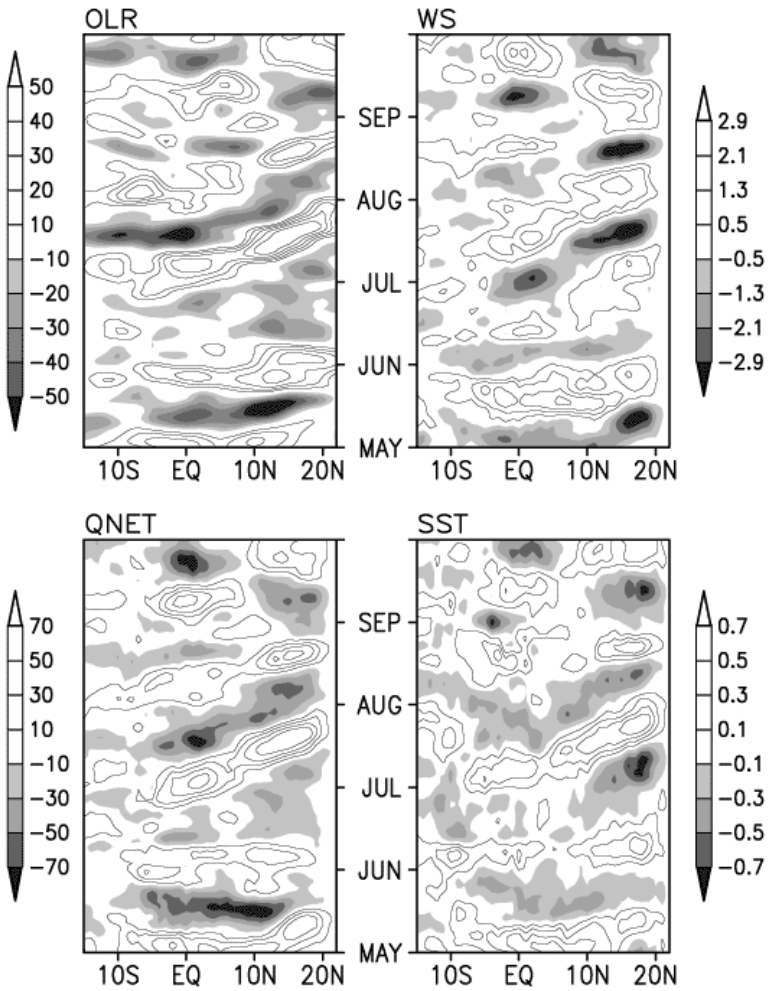

Figure 5.15. Time–latitude sections of 10–80-day filtered anomalies of OLR (Wm^{-2}), windspeed (ms^{-1}), net surface heat flux (Wm^{-2}), and SST (°C) averaged over 85°–90°E in the summer of 1998.
From Sengupta *et al.* (2001).

In terms of theoretical constructions for the boreal summer ISO, one of the most important distinctions or additions that need to be accounted for over the MJO is the ISO's northward propagation and the off-equatorial westward propagation of large-scale disturbances within the planetary-scale eastward moving structure (Figures 5.4 and 5.6). The earliest hypotheses regarding northward propagation did not require or account for any aspect of zonal asymmetry in the ISO pattern – which at that point was probably not that well defined. For example, Webster (1983) suggested that positive surface sensible heat flux anomalies into the atmosphere,

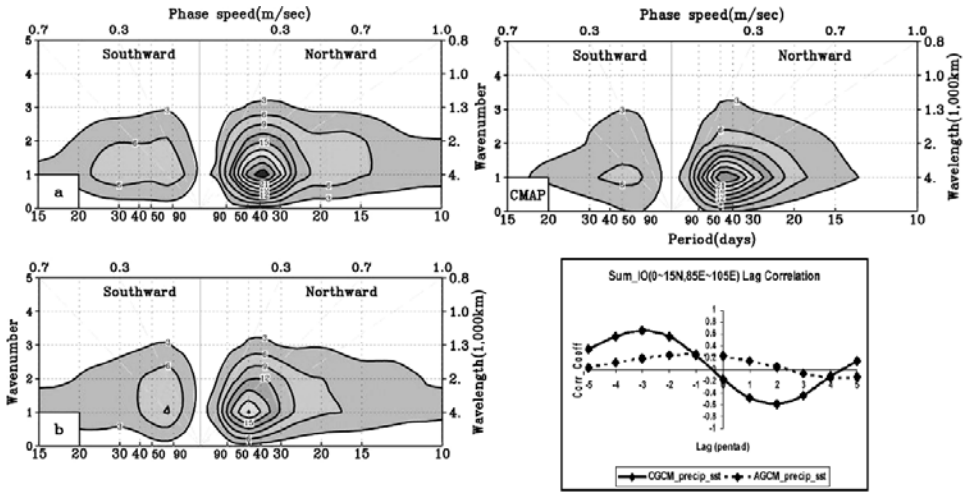

Figure 5.16. (Contour plots from Fu and Wang, 2004) Wavenumber–frequency power spectra of north–south propagation characteristics of rainfall from longitude range 65°E–95°E from a (U. Hawaii) CGCM (*upper left*), the corresponding AGCM using SSTs specified from the CGCM simulation (*lower left*), and CMAP rainfall data (Xie and Arkin, 1997) (*upper right*). (Line plots from Zheng *et al.*, 2004) Lagged correlation values between SST and rainfall anomalies averaged over 85°–105°E, 0°–15°N from a (GFDL) CGCM (solid line) and the corresponding AGCM using SSTs specified from the CGCM simulation (dotted line).

driven by ground temperature anomalies to the north of the convection, could destabilize the atmospheric column and promote northward movement of the convection. Gadgil and Srinivasan (1990) and Nanjundiah *et al.* (1992) suggested a similar mechanism but in their case it was the gradient in *moist* static energy that promoted the northward propagation. Based on a zonally symmetric model, Goswami and Shukla (1984) suggested that the interaction between convection, dynamics, and ground surface evaporation (the model oscillation diminished considerably over the ocean) can result in an oscillatory behavior of about the right timescale.

Inclusion of wave-like features and zonal asymmetry to the problem started with Lau and Peng's study (1990), which, based on numerical experiments, showed that the interaction between equatorial moist Kelvin waves could interact with the large-scale monsoon flow and produce quasigeostrophic baroclinic waves that would influence the south-east Asian region. The study by Hsu and Weng (2001) suggests that the north-westward propagating disturbances within the ISO complexes could develop from the interaction of an eastward propagating (MJO-like) convective disturbance and a subtropical westward propagating low-level convergence anomaly. As alluded to earlier, the combined works of Wang and Xie

(1997), Xie and Wang (1996), and Kemball-Cook and Wang (2001) help to explain some aspects of both the overall northward propagation of the large-scale complex and the westward moving variability embedded within it. Their studies suggest that as the near-equatorial ('MJO-like') convective complex moves eastward, with its attendant equatorial Kelvin and off-equatorial Rossby wave circulations, it develops weakened states upon encountering the heterogeneous Maritime Continent and the cooler central Pacific (Figure 5.6). At these stages, the relaxation process results in the emanation of north-westward propagating Rossby wave disturbances that account for the overall north-west–south-east tilt of the ISO 'rain bands' (Figure 5.4). Additional observational evidence for the connection between the emanation of Rossby waves and the rain band tilt was found by Annamalai and Slingo (2001) and Lawrence and Webster (2002). The eastward movement of these tilted rain bands thus results in a northward propagating feature when considered at a given longitude. Thus while most of the studies discussed above specifically tried to address the northward propagation of individual disturbances/rain bands, yet did not account for the overall structure and propagation of the ISO, they provided the latter but did not address why a given (Rossby wave) disturbance within the ISO complex has a northward propagating component.

Recently, the studies of Drbohlav and Wang (2004) and Jiang *et al.* (2004) have provided some possible answers to this question. Using much of the same model framework associated with the 'frictional CID' MJO analysis described above, but taking into account the strong easterly vertical shear occurring over the Asian monsoon region, these studies each concluded that this shear is a fundamental driver in the northward propagation. The easterly shear, along with the meridional gradient in vertical motion (i.e., ascending within the convective region and descending to the north), combine to form a vorticity twisting term that promotes the northward movement of the disturbed (i.e., cyclonic vorticity) regions. While the influence of easterly shear on northward propagation appeared crucial in these two studies, as well as in a GCM study (Kemball-Cook *et al.*, 2002), the study by Jiang *et al.* also indicated important contributions for promoting northward propagation from meridional advection of the low-level humidity gradient and from interactive SST. The nature of the latter process was discussed above and its importance to the development of northward propagation is also evident in the studies by Fu *et al.* (2003) and Fu and Wang (2004).

The discussion in this section is meant to highlight the theoretical developments associated with tropical subseasonal variability, namely the MJO/ISO phenomena (some treatment of the 10–20-day mode can be found in Goswami (2005)). While there is yet to be overall agreement on a given theory, it appears that most of the essential issues that need to be considered in developing and refining our theories have at least been identified. This achievement at least provides the means for the theory to help guide GCM model diagnosis and development aimed at improving their representation of the MJO/ISO, which, as will be discussed in the next section, remains an ongoing challenge.

5.6 NUMERICAL MODELING

Previous sections have outlined our observational and theoretical understanding of tropical ISV. At this point it is clear that the ISV, namely in the form of the ISO, is an inherent mode of variability within the Asian summer monsoon system, one that dictates its active and break periods, modulates the embedded synoptic variability, and possibly even helps to determine its interannual variability. In addition, the previous section suggests that we have gained considerable appreciation for the essential physical processes involved in its maintenance and evolution. Yet, in order to substantiate and further our theoretical understanding of the ISO, take advantage of what it can offer in terms of short-term monsoon prediction, ensure that our weather forecasts and climate simulations/predictions include all the necessary and important scale interactions, it becomes imperative to be able to simulate ISV in a numerical setting. Consistent with most of the topics discussed above, a majority of the research and development in this area has been done in association with the MJO. However, given the overall similarities between the MJO and the ISO, particularly in regards to their modeling successes and shortcomings, this chapter will focus primarily on boreal summer activity. In particular, it will tend to only highlight the state-of-affairs of ISO modeling, focusing on the main shortcomings and the recent attempts to overcome them. Keep in mind that some of the findings discussed in previous sections were derived from GCM studies and thus part of the material related to numerical modeling of the ISO has been discussed above. For a more thorough review of modeling issues related to both the MJO and ISO, the reader is referred to Slingo *et al.* (2005).

As discussed in the previous section, the theoretical understanding of the ISO is a more challenging prospect than that for the MJO. This is primarily due to the more complex mean flow that the ISO interacts with compared with the MJO, as well as the greater heterogeneity of the underlying surface conditions and topography in the Asian monsoon sector relative to the equatorial Indian and western Pacific Oceans where the MJO is most prominent. From this standpoint, it is not surprising that as difficult as it has been to simulate the MJO in numerical settings (Lau and Lau, 1986; Park *et al.*, 1990; Slingo and Madden, 1991; Slingo *et al.*, 1996; Wang and Schlesinger, 1999; Hendon, 2000; Inness *et al.*, 2001; Maloney and Hartmann, 2001; Maloney, 2002; Wu *et al.*, 2002; Inness and Slingo, 2003; Inness *et al.*, 2003; Lee *et al.*, 2003; Liess and Bengtsson, 2003; Liess *et al.*, 2003; Waliser *et al.*, 2003a; ECMWF, 2004), it has been even more infrequent that reasonable simulations of the ISO have been noted. Prominent shortcomings highlighted in the above MJO GCM studies include a tendency for weak variability, disturbances that tend to propagate too fast, sensitivity to mean state conditions – particularly in the Indian and western Pacific Ocean, a less than ideal representation of the modulation by the annual cycle, and in some cases improper phase relationships between convection and surface heat flux components. While some of these shortcomings hold for the ISO, recent diagnostic studies of the ISO in GCMs indicates that there are a number of problems that tend to be unique to the boreal summer activity.

In their examination of dynamical seasonal prediction of the Asian summer

monsoon, the study by Sperber *et al.* (2001) also included an assessment of how well seven AGCM models reproduced subseasonal modes of variability. Their results showed that for many models, the dominant dynamical pattern of subseasonal variability (i.e., dynamical analog to Figure 5.4), as depicted in observations, is reasonably well simulated. Beyond this however, the AGCMs had difficulty in representing the pattern of precipitation associated with the dominant mode (e.g., Figure 5.4) as well as difficulty in simulating most aspects of the higher order modes of subseasonal variability. In addition, that study found that the models usually failed to project the subseasonal modes onto the seasonal mean anomalies, even in cases where the mode may have been influenced by surface boundary conditions (see discussion in Section 5.4.1).

The study by Waliser *et al.* (2003e) examined ten AGCM simulations to assess their representation of ISO variability associated with the Asian summer monsoon. Figure 5.17 shows the spatial patterns of boreal summer ISV in the ten AGCMs analyzed and the observations. Evident is the very wide range of realism depicted by the models, with a couple of the models having virtually no ISV and a few having ISV that exceeds that exhibited in observations. In some cases, the spatial pattern of variability is somewhat realistic, at least away from the equator. Not surprising is the result that when considering maps such as that in Figure 5.17 for both winter and summer, the fidelity of a model to represent northern hemisphere summer vs. winter ISV appears to be strongly linked. In addition, their analysis showed that most of the model ISO patterns did exhibit some form of northward propagation. Figure 5.18 (color section) shows composite ISO patterns from the observations and seven of the ten AGCMs analyzed. While the seeds of northward propagation are apparent, the model ISO patterns are typically less coherent, lack sufficient eastward propagation, have smaller zonal and meridional spatial scales than the observed patterns, and are often limited to one side or the other of the Maritime Continent. In addition, for those models that do exhibit a large-scale variability, they often have a south-west–north-east tilt rather than the observed north-west–south-west tilt.

One of the most pervasive and problematic feature of the models' depiction of the ISO is the overall lack of variability in the equatorial Indian Ocean. In some cases, this characteristic appears to result due to the propensity of a number of models to form double convergence zones about the equator rather than one region of strong convergence on the equator. This shortcoming not only results in a poor representation of the local rainfall pattern but is also found to significantly influence the models' representations of the global-scale teleconnection patterns associated with the ISO (e.g., Figure 5.10). The results of Zheng *et al.* (2004) indicate that the lack of ocean coupling in the above AGCM simulations may be at least part of the reason for their reduced levels of ISV in the Indian Ocean. And, as discussed in the previous section, the results of Kemball-Cook and Wang (2002), Fu *et al.* (2003), and Fu and Wang (2004) all suggest that improvements in a model's representation of the northward propagation of the ISO can result from the inclusion of ocean coupling.

In another related study to the ISO, Kang *et al.* (2002b) examined how well AGCMs (the same ten as in the Waliser *et al.* (2003e) study discussed above)

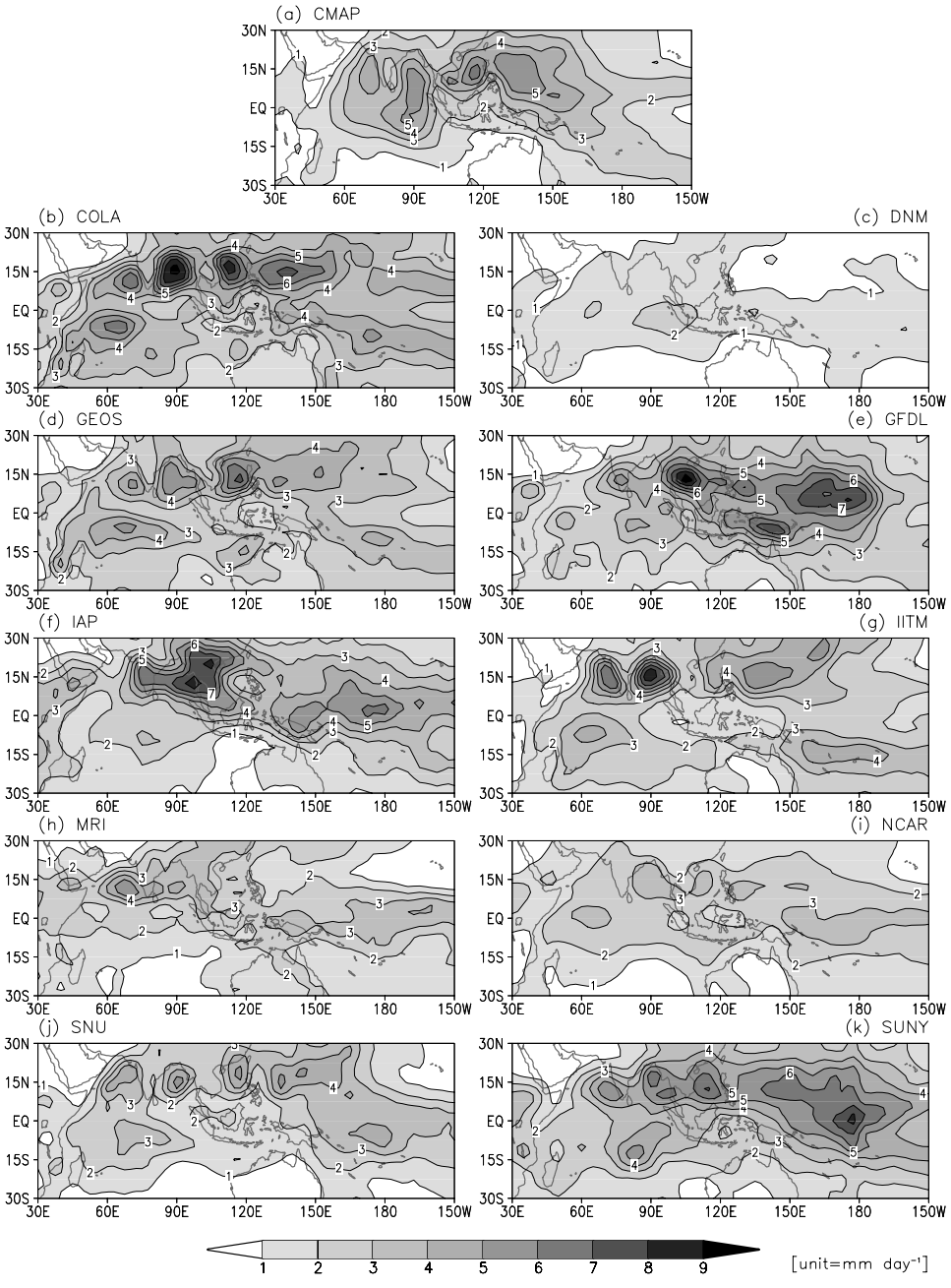

Figure 5.17. Standard deviation of 20–90-day filtered rainfall (mm day^{-1}) for Boreal from the CMAP observations (Xie and Arkin, 1997) (*top*) for 1979 to 1998 and for the ten AGCMs (*lower*). In the case of the models, there were 20 summer seasons of data (i.e., ten members each consisting of two years). From Waliser *et al.* (2003e).

simulate the climatological intraseasonal variation of the Asian summer monsoon (Section 5.2.4). Based on an EOF analysis of the high-frequency seasonal progression of the monsoon, their analysis showed that all the models generally failed to faithfully simulate the CISO. While this is certainly related to the models' poor representation of the ISO, it is also necessarily related to the lack of any model to realistically represent the slowly evolving seasonal pattern of monsoon rainfall. In addition, their study showed that the simulated northward propagation of the climatological intraseasonal oscillations (CISO) of precipitation occur 20–30 days earlier than the observations over the east Asian monsoon region. This result is in partial agreement with the studies by Wu *et al.* (2002), Fu and Wang (2004), and Zheng *et al.* (2004) which all indicate that for individual ISO events, the lag between positive SST anomalies and convection is reduced by about 5–10 days in AGCM simulations relative to the observations and CGCM simulations. One of the most important implications of this latter result is that if specified SSTs are used in a prediction environment, phase errors in tropical convection of the order of 5–10 days (or 5°–20° longitude) will occur. This is substantial when considering the local tropical prediction but also problematic when considering the impact on the extratropics. Thus, subseasonal (e.g., MJO/ISO) predictions must include ocean coupling (i.e., a 'two-tier' prediction framework is inadequate).

Based on the above brief summary of the state-of-affairs of ISO modeling, it is clear that a number of critical problems remain to be solved. Recognition of the need for better ISO simulations and the associated benefits that could be derived from accurate predictions, has led to some concerted efforts to try and remedy these problems. In June of 2003, a modeling workshop was held on MJO/ISO modeling (Waliser *et al.*, 2003a; see also ECMWF, 2004) to assess current capabilities, recent developments, and to determine future directions. From the workshop presentations and the results such as those discussed above, the following summarizing remarks in terms of modeling can be made. In contrast to a decade ago (e.g., Slingo *et al.*, 1996), specific model problems are not as generic. For example, many models have variability stronger than observed or even have propagation speeds than are slower than observed. In addition, there seems to be more models getting something in the way of an MJO/ISO, and fewer models that are completely absent of ISV phenomenon. Unfortunately, when a model does exhibit a relatively good MJO/ISO, we can at best only give vague or plausible explanations for its relative success. This inhibits the extension of individual model successes to other more ISV challenged models.

It has long been thought that the ISV problem likely relates to the treatment of the cumulus convection. This is because typically the greatest sensitivity that the MJO/ISO simulation exhibits to various model 'tunings' is associated with that of the convective parameterization – or closely related processes (e.g., Slingo *et al.*, 1996; Wang and Schlesinger, 1999; Lee *et al.*, 2001; Maloney and Hartmann, 2001; Maloney, 2002; Lee *et al.*, 2003). This was fairly evident from many of the presentations in the MJO/ISO modeling workshop mentioned above, which included a number of efforts illustrating that it was somewhat possible to 'tune in' better ISV via modifications such as the Tokioka 'fix' to the Arakawa-Schubert parameterization (Tokioka *et al.*, 1988), boundary layer inhibition, controls on free atmospheric

humidity, inclusion of gustiness, etc. While we still grapple with why certain changes lead to a better or worse MJO, it is expected or perceived that a more realistic parameterization of convection, or 'no' parameterization at all (Randall *et al.*, 2003; Kuang *et al.*, 2004), should/will lead to more realistic MJO simulations. In addition to the convection issue, it seems more of a certainty that SST coupling does play an important role in the quality of a MJO/ISO simulation. However, for this interaction to be properly represented, it is imperative the surface heat flux anomalies (mainly short-wave and latent) associated with the MJO/ISO be reproduced with some fidelity. This in turn involves the representation of clouds and the interactions between the heating profiles and the surface in producing a realistic boundary layer.

In regards to observations and their use in model development and improvement, it is clear that we have enough data to determine that our GCMs have poor ISV representations but probably not enough information to properly tune the models or to remove ambiguities regarding parameterization choices. At this stage, the most notable areas where we lack important constraining/verifying information are associated with the hydrological cycle (e.g., moisture, re-evaporation, microphysics, latent heating profiles) as well as boundary layer processes and cloud–radiative interactions. For example, how well do we represent the partition between deep and shallow heating associated with the MJO/ISO life cycle (e.g., Wu, 2003)? In addition, and as alluded to in Section 5.5.1, it is still to be determined how much cloud long-wave forcing influences the instability of the atmosphere during the convective phase of the MJO/ISO? Additional modeling problems that have to be rectified include achieving a proper representation of the basic state. Issues such as the tendency for models to produce double ITCZs, produce inadequate representations of the mean monsoon or the surface zonal wind structure in the Indo-Pacific warm pool, or exhibit biased coupled basic states can all produce limitations on the fidelity of a model's ISV representation. These basic state issues are extremely important in the forecasting context, discussed in the next section, since the models need to be initialized to the observed state but then will subsequently undergo an adjustment toward their own (poor) basic state which can wreak havoc on the forecasts.

5.7 PREDICTION AND PREDICTABILITY

As our understanding and modeling capabilities of ISV grow, it is natural to want to exploit this knowledge and ability in order to develop improved and expanded monsoon prediction resources. This section will review developments made regarding our capabilities for predicting tropical ISV, specifically the MJO/ISO, via empirical and dynamical means, our understanding of its predictability characteristics and present efforts at real time prediction. A more complete review of this material can be found in Waliser (2004).

5.7.1 Empirical models

By the late 1980s, many characteristics of the ISV were fairly well documented and it was clear that the dominant modes of ISV exhibited a number of reproducible features from one event to another and in events between years. Since numerical weather and climate models typically had a relatively poor representation of the ISV at the time, a natural avenue to develop was the use of empirical models. The first study along these lines was by von Storch and Xu (1990) who examined POPs (Hasselmann, 1988) of equatorial 200-hPa velocity potential (VP200) anomalies. They found that forecasts based on the first pair of POPs, which tended to emphasize the MJO, produced forecasts that had useful skill out to about 15 days. While this was an encouraging result, at least relative to 'weather', the limited length of data used ($\sim$5 yr) combined with the non-stationary characteristics of the MJO over interannual timescales (e.g., Section 5.3) necessitated some caution in over-interpreting it. Moreover, given the smoothly varying nature of VP200, and the fact that it is only loosely related to near-surface meteorological variables (e.g., precipitation), also suggested caution in generalizing this result to other years, variables, and/or different techniques. A number of years later, Waliser *et al.* (1999b) developed an empirical ISV forecasting method in order to benchmark numerical long-range forecasts and to begin exploring the feasibility of employing such a model to augment operational long-range forecasting procedures. The model was based on singular value decomposition (SVD) and used previous and present pentads of filtered OLR to predict future pentads of OLR. Separate models were developed for northern hemisphere winter and summer conditions and each exhibited temporal correlations against observed total anomalies of the order of 0.3 to 0.5 over the eastern hemisphere. While this result also promoted some optimism for making subseasonal predictions, the fact that the model utilized filtered data warranted caution and limited its immediate real time applicability.

Following the above were a number of empirical MJO forecasting efforts that each produced a unique and useful approach to the problem. For example, Lo and Hendon (2000) developed a lag regression model that uses as predictors the first two and first three principal components of spatially and intraseasonally filtered OLR and 200-hPa streamfunction (φ200), respectively, to predict the evolution of the OLR and φ200 anomalies associated with the MJO. Separate methods were used to remove the annual cycle, interannual, and high-frequency (i.e., $<$30 days) components, leaving only the ISV. When tested on independent data, the model exhibited useful skill for predictions of these principal components over at least 15 days, with greater skill during active vs. quiescent MJO periods. A somewhat different approach was taken by Mo (2001) who utilized empirical basis functions in time for the forecasting procedure. This was done by using a combination of singular spectrum analysis (SSA; Vautard and Ghil, 1989) for the filtering and identification of the principal modes of variability and the maximum entropy method (MEM; Keppenne and Ghil, 1992) for the forecasting component. The procedure was applied to monitor and forecast OLR anomalies (OLRAs) associated with the MJO, intraseasonal modes associated with the Asian monsoon, and

variability related to both of these that occurs over the US west coast. When tested on independent December–February and June–August OLRA data, the averaged correlation over the tropics between the predicted and the observed anomalies was 0.65 at the lead times of four pentads (20 days).

In a quite different approach, Wheeler and Weickmann (2001) utilized tropical wave theory (Matsuno, 1966) as the basis for their filtering and forecasting technique. Essentially, a space–time Fourier analysis is performed on daily OLR data for a given time–longitude section of interest in the tropics. In a previous study, Wheeler and Kiladis (1999) showed that the spectrum from such an analysis exhibits variability that is associated with the modes that one would expect from theoretical considerations (e.g., Kelvin, mixed Rossby–Gravity waves), as well as the expected peak of variability around wavenumbers 1–3 and 40–60 days associated with the MJO. In order to monitor and predict the evolution of a given mode of interest, the specific zonal wavenumbers and frequencies associated with the mode(s) of interest are retained and then the modified spectrum is inverse Fourier analyzed. The filtered values obtained for times before the end of the dataset are used for monitoring the activity of a given mode, while the filtered fields obtained for times after the end point may be used as a forecast. For prediction, the method exhibits useful skill for the MJO over about 15–20 days. An advantage is that the method readily provides predictions of other well-defined, typically higher frequency, modes of large-scale tropical variability, although it has little applicability to the Asian monsoon.

In an effort that focused on active and break conditions of the Indian summer monsoon, Goswami and Xavier (2003) noted that all active (break) conditions go over to a break (active) phases after about 15–20 days – albeit with a fair amount of event-to-event variability. Using a rainfall-based ISO index and a definition of active and break conditions, they calculated the typical (i.e., ensemble average) transition from active to break (and break to active) conditions as a function of lead time. This method exhibited apparent skill in predicting break-to-active (active-to-break) transitions over about 10 (20) days lead time, indicating that monsoon breaks are intrinsically more predictable than active monsoon conditions. Similar results in this regard were found by (Waliser *et al.*, 2003d) using an ensemble of twin-predictability GCM experiments (discussed below).

The above discussion gives a flavor of the types of empirical forecast models for ISV that have been developed to date. A number of additional approaches presently associated with real time efforts are discussed below. It is worth emphasizing that as yet numerical forecast models have not demonstrated the skill level associated with the above techniques. Moreover, it is worth reiterating that in no cases are these particularly complex techniques and thus it its likely that we may not develope models that have saturated the skill potential for empirical methods. In addition, it is also worth highlighting that ISV-related events are at best quasiperiodic, meaning conditions can be relatively quiescent and then an event suddenly develops. Each of the models above would tend to perform relatively poorly at forecasting this initial development, as they all tend to rely on the periodic nature of ISV to forecast its evolution. For these scenarios, as well as for dealing with the

inhomogeneity of ISV events, it will be vital to improve our dynamic models, as they are likely to be the best means to deal with these sorts of issues.

5.7.2 Dynamical forecast models

As yet, there have only been a handful of studies that have examined forecast skill (i.e., verified against observations) from dynamical models. This has probably stemmed from what amounted to considerably less overall interest in forecasting the intraseasonal timescale relative to weather and ENSO, the difficulty and resources required to produce an adequate sample of very long-range weather forecasts (at least 30 days), the pessimism and known challenges associated with tropical weather forecasting in general, and the indications that neither our forecast or climate simulation models were not very adept at simulating ISV. In any case, as part of a more generalized forecast skill study of the planetary-scale divergent circulation, Chen and Alpert (1990) examined MJO forecast skill from one year (June 1987–May 1988) of daily 10-day forecasts from the US National Meteorological Center's (NMC; now National Centers for Environmental Prediction (NCEP)) medium range forecast (MRF) model in terms of the VP200. In their analysis, the MRF's forecast skill, measured in terms of spatial correlations of VP200 between 50°N–50°S, declined to about 0.6 by forecast day 6 and 0.4 by forecast day 9. This relatively poor skill was attributed to: (1) the inability of the model to maintain MJO variability during a forecast, and (2) the model's tendency to propagate MJO anomalies too fast. Lau and Chang (1992) analyzed one season (14 Dec 1986–31 Mar 1987) of daily 30-day global forecasts derived from a set of Dynamical Extended Range Forecasts (DERFs) from a research version of the MRF model mentioned above. Their results showed that the forecast model had significant skill in predicting the global pattern of ISV in VP200 and streamfunction for up to 10 days lead time, with the error growth of tropical and extratropical low-frequency modes less than persistence when the amplitude of the MJO was large and vice versa when the amplitude was small.

Both Hendon *et al.* (2000) and Jones *et al.* (2000) analyzed a more recent DERF experiment which used the reanalysis version (Kalnay *et al.*, 1996) of the NCEP MRF model (Schemm *et al.*, 1996). This experiment included 50-day forecasts made once a day for the period January 1985 to February 1990. In both studies, the focus was on the MJO. Using different analysis and filtering techniques for identifying the MJO within the forecasts and thus for assessing forecast skill against observations, both studies concluded that this version of the NCEP MRF model still exhibited rather poor MJO forecast skill. Specifically, Jones *et al.* found that the anomaly correlations of intraseasonally filtered values of 200-hPa zonal wind, zonally averaged along the equator, declined from about 0.6 on day 3 to 0.2 by day 10 with some indication that the forecast skill was slightly better (worse) when the MJO was particularly active (weak). The rather poor forecast skill was attributed to the development of systematic errors in the forecast upper level winds, particularly over the eastern Pacific and, as above, due to the inability of this model to maintain/simulate a robust MJO phenomena itself. The analysis by Hendon *et al.*

showed that forecasts initialized during very active episodes of the MJO did not reproduce the observed eastward propagation of the tropical convection and circulation anomalies, rather the anomalies would typically weaken in places and even retrograde in some cases. Typically it was found that the convective anomalies would decay almost completely by day 7 of the forecast, and in nearly the same time considerable systematic errors in the extratropical 200-hPa streamfunction would develop. The above studies point to the need for the forecast models to not only have a proper representation of MJO anomalies but also to produce an unbiased mean state so initialization errors and their subsequent evolution/adjustment don't contaminate the forecast over these relatively long lead times.

The most prominent studies of forecast skill associated with the boreal summer ISO were based on the work of T. N. Krishnamurti in the early 1990s. In the first study, Krishnamurti *et al*. (1990) laid the groundwork for the method which argues that part of the loss of forecast skill associated with 'low-frequency modes' comes about from the errors and evolution of high wavenumber/frequency variability. If the objectives are the prediction of active and break monsoon periods, then it is plausible to filter the initial state in order to remove all but the recent (e.g., 45-day) 'mean' state and the low-frequency modes of interest (in this case, obtained via time filtering). Krishnamurti *et al*. argue that this will delay the 'contamination of the low-frequency modes as a result of the energy exchanges from the higher frequency modes'. This idea was tested in forecasts that used observed SST anomalies, filtered to include only 30–50-day variability. While the latter specification certainly provided the hindcast with information that a true forecast would not have, the results from the case study performed for 31 July 1979 were still encouraging. They showed that the model forecast exhibited considerable skill at predicting the meridional motion of the 850-mb trough–ridge system over Indian and the eastward propagation of the 200-mb divergence anomaly out to about 4 weeks. In Krishnamurti *et al*. (1992a, 1995), analogous experiments using two select case studies were performed for low-frequency 'wet and dry spells' over China and Australia for each of their associated summer monsoons with similar results. As in the first study, the SST anomalies were found to be vital to retaining the forecast skill. In both of these studies, simple empirical prediction of the SST anomalies was incorporated and found to provide much of the necessary SST information to retain most of the long-lead forecast skill found in this suite of experiments (see Fu and Wang, 2004; Zheng *et al*., 2004).

5.7.3 Predictability

The research highlighted in the previous two sections provides an indication of what the inherent predictability limit might be for principal modes of ISV. From the empirical model studies, this limit might be ascertained to be around 20–30 days. However, most empirical models are limited in the totality of the weather/climate system they can predict, their ability to adapt to arbitrary conditions, and their ability to take advantage of known physical constraints. Thus, one might conclude

that if dynamical models had a realistic representation of ISV, this limit might be extended. However, the information that can be ascertained from the above dynamical studies is limited due to the facts that they were either based on models with a relatively poor representation of ISV, they were based on only a few select cases, and since they were based on verification between models and observations all include model systematic bias in addition to the natural non-linear processes that limit predictability.

A complimentary avenue of research for ascertaining the inherent limits of prediction for ISV was taken by Waliser *et al.* (2003c, 2003d) who used so-called 'twin predictability' experiments. In this case, the model employed is presumed to be 'perfect' and forecast experiments are verified against others that only differ in the initial conditions (e.g., Lorenz, 1965; Shukla, 1985). The important consideration for a study such as this is that the model provides a relatively realistic representation of the phenomenon of interest. In this case, the experiments were performed with the NASA Goddard Laboratory for Atmospheres (GLA) GCM (Kalnay *et al.*, 1983; Sud and Walker, 1992). In a number of studies, this model has been shown to exhibit a relatively realistic ISV representation (Slingo *et al.*, 1996; Sperber *et al.*, 1997; Waliser *et al.*, 2003e) with reasonable amplitude, propagation speed, surface flux properties, seasonal modulation, and interannual variability (Waliser *et al.*, 2001). For these studies, a 10-year control simulation using specified annual cycle SSTs was performed in order to provide initial conditions from which to perform an ensemble of twin predictability experiments. The following discussion describes the boreal summer ISO study (Waliser *et al.*, 2003d) but the methods and results are quite similar for the MJO (Waliser *et al.*, 2003c). Initial conditions were taken from periods of strong ISO activity identified via EOF analysis of 30–90-day band-passed tropical rainfall during the May–September season. From the above analysis, 21 cases were chosen when the ISO convection was located over the central Indian Ocean, northern Indian Ocean, south-east Asia region, and north-west tropical Pacific, respectively, making 84 cases in total. Two different sets of small random perturbations, determined in a rather *ad hoc* and simplistic manner, were added to these 84 initial states. Simulations were then performed for 90 days from each of these 168 perturbed initial conditions.

A measure of potential predictability was constructed based on a ratio of the signal associated with the MJO, in terms of band-passed (30–90 day filter) rainfall or VP200 (VP200), and the mean square error between sets of twin (band-passed) forecasts. Predictability was considered useful if this ratio was greater than one, and thus if the mean square error was less than the signal associated with the MJO. The results indicate that useful predictability for this model's ISO extends over about 20–30 days for VP200 and about 10–15 days for rainfall (Figure 5.19). This is in contrast to the timescales of useful predictability for the model's weather that is about 12 days for VP200 and 7 days for rainfall. Predictability was shown to be sensitive to the amplitude of the events, with stronger events being more predictable. In addition and as indicated above, the predictability measure indicated greater predictability for the convective phase at short ($<\sim$5 days) lead times and for the suppressed phase at longer ($>\sim$15 days) lead times.

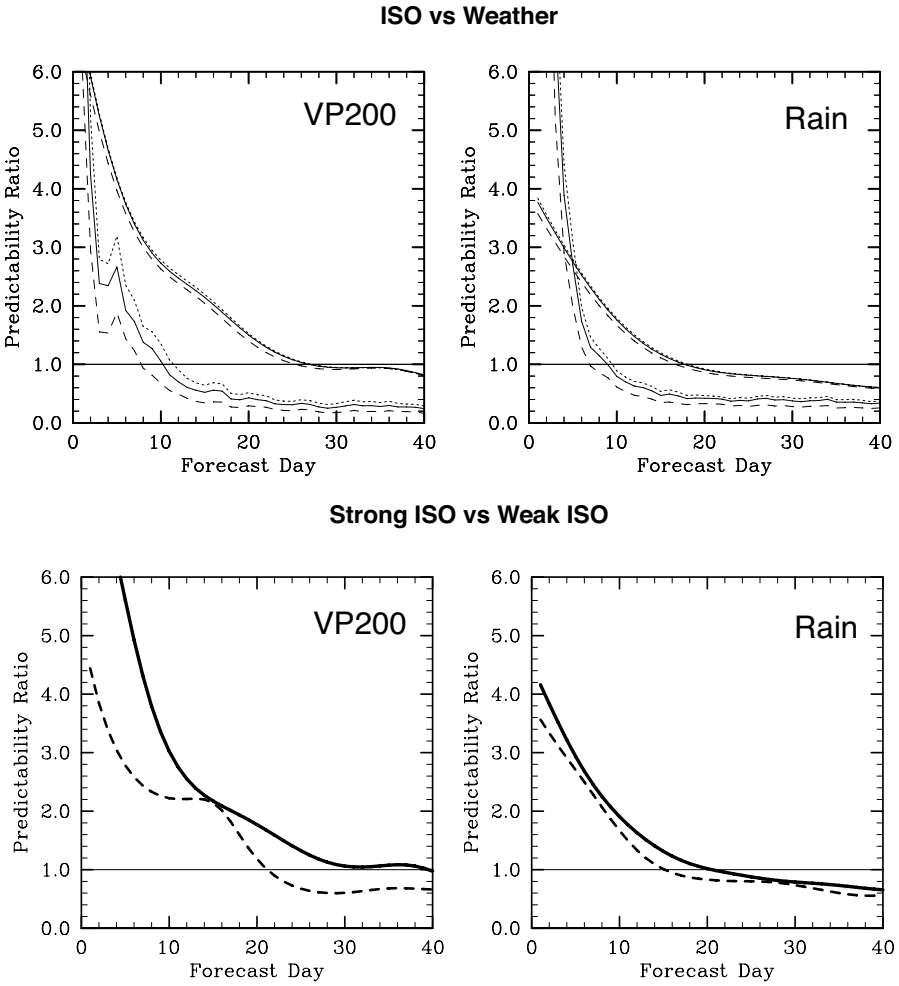

Figure 5.19. (*top*) ISO predictability vs. lead time for 200-hPa velocity potential (VP200; *left*) and rainfall (*right*) averaged over the region 4°N–24°N and 72.5°E–132.5°E. The results are based on all 168 northern hemisphere summertime cases from the dynamical forecasts. The rightmost (leftmost) group of lines are based on an evaluation using filtered (unfiltered) data to ascertain the predictability of the model's ISO (weather). (*bottom*) Same as (*top*), except that the solid (dashed) lines are based on forecasts using the 80 strongest (weakest) ISO cases.

In order to address the sensitivity of the above results to the model used and the analysis framework, an analogous study has recently been undertaken by Liess *et al.* (2004) using the ECHAM AGCM. The modeling and analysis framework is similar to that described above with two important exceptions. First, rather than select a large number of events (i.e., ~15–20) for each of the four phases of the ISO (i.e., as it propagates north-eastward) and performing two perturbation experiments for each,

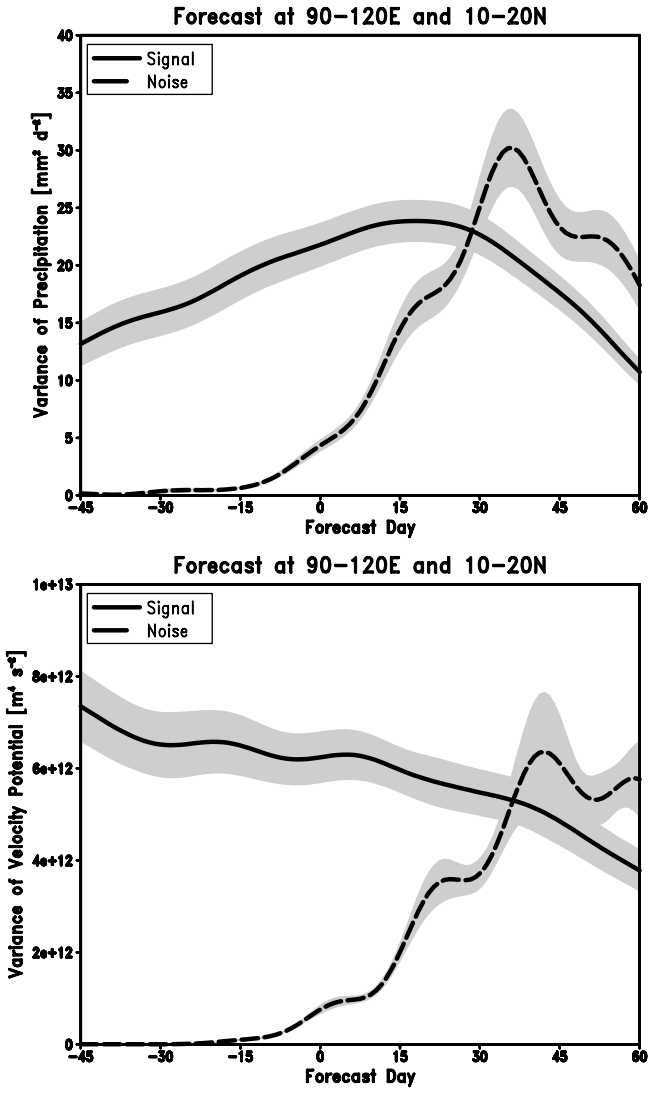

Figure 5.20. Signal-to-noise ratio of 30–90-day filtered precipitation (*top*) and 200-hPa velocity potential (*bottom*) predictions averaged over all four phases of three ISO events. Shadings represent the significance at the 95% interval based on all 12 15-member ensemble forecasts. All values are averaged over the region 90°–120°E and 10°–20°N.
Adapted from study by Liess *et al.* (2004).

this study has selected the strongest 3 events and performed a 15-member ensemble for each of the four phases. In addition, rather than use simply determined perturbations, this study uses the breeding method (Toth and Kalnay, 1993; Cai *et al.*, 2003). Figure 5.20 shows the combined results from all 12 15-member ensemble ISO

forecasts using the ECHAM5 AGCM. The data for the figure are taken from 90°E to 120°E and 10°N to 20°N for 30–90-day band-pass filtered rainfall (upper) and VP200 (lower) anomalies. These results suggest that the boreal summer MJO has dynamical predictability with lead times potentially up to and beyond 30 days. These lead times are at least as large, if not larger, than those found in Waliser *et al.* (2003c,d) studies highlighted above. However, it should be noted that the event analysed here is a particularly robust and strong one for the model, and those above were based on both strong and moderate sized events which could account for the difference. In any case, even though the above results do not take into account systematic model bias relative to the observations, they, along with many of the other studies discussed above, indicate that a promising avenue and timescale of operational monsoon prediction lies ahead.

5.7.4 Real time forecasts

Based on the qualified success of some of the prediction efforts discussed above, a number of forecast schemes have been implemented in real time. The first of these was associated with the Wheeler and Weickmann (2001) scheme described in Section 5.7.1[1] and is thus more strictly associated with the MJO as well as other coherent modes of tropical variability (e.g., Kelvin, mixed Rossby gravity). A second effort that has been developed more recently builds on the study by Lo and Hendon (2000) and utilizes what is referred to as an all-season real time multivariate MJO (RMM) index (Wheeler and Hendon, 2004).[2] The index results from projecting daily data onto the first two modes of a combined EOF of tropical OLR, and zonal winds at 850 and 200 hPa. This projection onto the EOF pair, along with the prior removal of an estimate of the data's very low-frequency components (e.g., ENSO) via their relationship to interannual SST variability, remove the need to perform time filtering to identify the MJO. The values of the index (actually two indices, one amplitude time series for mode 1 (RMM1) and one for mode 2 (RMM2)) at any given time can be used for monitoring. In addition, seasonally and time lag dependent regression can be used to forecast the evolution of these indices or any associated field, using as predictors RMM1 and RMM2 at the initial day. Skill scores in terms of spatial correlation are about 0.6 at 12-day forecast, and 0.5 for a 15-day forecast. The advantages of the method are that it has a seasonal dependence built in and it can be easily adapted for forecasting nearly any field.

Jones *et al.* (2004b) has also produced real time predictions of the MJO.[3] The scheme is based on band-passed (20–90 days) OLR, and zonal winds at 850 and 200 hPa. Upon filtering, a combined EOF of the three fields is computed and then the principle components (PCs) are separated into summer and winter. A seasonally dependent regression model is then formed at every given lead between 1 and 10 pentads. The model utilizes the first five PCs from the EOF analysis and the five most

[1] http://www.bom.gov.au/bmrc/clfor/cfstaff/matw/maproom/OLR_modes/index.htm
[2] http://www.bom.gov.au/bmrc/clfor/cfstaff/matw/maproom/RMM/index.htm
[3] http://www.icess.ucsb.edu/asr/mjo_forecasts.htm

recent values of the PCs. The model is found to exhibit winter and summer skills comparable to the other empirical models described in Section 5.7a.

In quite a different approach, stemming from a somewhat different and/or more comprehensive objective, Matt Newman and his colleagues have developed and implemented a real time forecasting scheme[4] that has applicability to the MJO based on what is often referred to as the Linear Inverse Model (i.e., LIM; Winkler *et al.*, 2001; Newman *et al.*, 2003). The LIM is based on NCEP/NCAR reanalysis data (Kalnay *et al.*, 1996) that has had the annual cycle removed, been smoothed with a 7-day running mean filter, gridded to T21 spatial resolution, and been reduced by EOF decomposition. The specific fields used include global 250 and 750-hPa streamfunction and tropical column integrated diabatic heating. For the northern hemisphere winter (summer) model, the first 30 (30) streamfunction and 7 (20) diabatic heating EOFs are used. In this model, historical data are used to define the relationship between a given state (i.e., a weekly average) and conditions one week later, with the process being iterated to produce multiweek forecasts. The advantage of the model is that it includes both tropical (in terms of diabatic heating – hence a prediction of the MJO) and extratropical (in terms of streamfunction) forecasts. In this way, the interaction between the two can be more readily examined and diagnosed. For tropical forecasts of diabatic heating, the LIM slightly outperforms a research version of the NCEP MRF model at lead times of 2 weeks, for both summer and winter.

It is almost a certainty that the greatest impact from ISV on society via direct impacts on day-to-day weather, agriculture, and associated economics is associated with the Asian summer monsoon. Motivated by this, Webster and Hoyos (2003) have developed an empirical model for predicting ISV in Indian district rainfall. The empirical model is physically based with predictors drawn from the composite structure of the boreal summer ISO (e.g., Indian Ocean SST, precipitation over India, upper level easterly jet). In essence, the model is Bayesian and uses a wavelet technique to separate significant spectral bands. The model illustrates considerable skill, even over 20–25 days, in predicting rainfall in hindcast mode. It was used for the first time during the summer of 2003 in a real time operational mode in the Climate Forecast Application in Bangladesh project. Since then, these forecasts of precipitation (and river discharge) have been integrated into the Bangladesh forecasting system on an experimental basis.

Based on the sorts of activities and success described above, along with the needs to take a more systematic approach to diagnosing problems in dynamical forecasts of the ISV, an experimental 'MJO' prediction program has recently been formulated.[5] The project's website has been operational since about late 2003 and is host to real time predictions of ISV from about 3–4 empirical methods and about 3–4 numerical forecast models. This effort continues to grow and evolve and during the winter and spring of 2004 began to also include 'synoptic' discussions of ISV conditions and their forecasts, with particular emphasis on the tropical–extratropical

[4] http://www.cdc.noaa.gov/map/images/mjo/
[5] http://www.cdc.noaa.gov/MJO/index.html

interactions. Additional information on this effort can be found in Waliser *et al.* (2003a) and Waliser (2005).

5.8 CONCLUSION

The literature reviewed here has shown that tropical intraseasonal variability makes up an extremely important part of the character and evolution of the Asian summer monsoon. While its most pronounced influence is associated with its direct connection to monsoon active and break periods, other important effects include its modulation of higher frequency variability and the role it may play in helping to determine interannual and longer term variability. A principal driver of the present enthusiasm for the subseasonal component of the monsoon is it offers a new – relative to the longstanding efforts at seasonal prediction – and unique form of predictive capability that is just beginning to be exploited. The principle roadblock to achieving the full potential that such predictability might offer is the development of a more robust and well-understood modeling capability, one that can withstand even modest observational scrutiny. Recent years have seen tangible progress in the form of theoretical hypotheses through the identification and narrowing of the major physical processes underlying ISV, as well as the acquisition of a wide variety of new data sets and field programs. The latter includes BOBMEX (Bhat *et al.*, 2001), JASMINE (Webster *et al.*, 2002), GAME-GEWEX (GAME, 1998), SCSMEX (Lau *et al.*, 2000), the CLIVAR/GCM Monsoon Intercomparison Project (Kang *et al.*, 2002a; Waliser *et al.*, 2003e), the development of an Indian Ocean moored array and drifter program (Meyers and Wijffels, 2004), as well as a number of new and exciting satellite programs (e.g., TRMM, AIRS, MODIS, MISR). At least in terms of intraseasonal variability of the monsoon, these additional resources and theoretical developments should make the coming decade a promising and productive one that will hopefully lead to a greatly improved modeling and predictive capability.

Relatively large uncertainties and/or gaps in our knowledge still exist in terms of the manner high-frequency (e.g., 10–30-day) and intraseasonal (40–60-day) variability interact, how ENSO or other low-frequency variations can modify ISV, and in turn, the degree that ISO variations contribute to interannual variability and the extent that this is chaotically driven. Theoretical and GCM efforts still struggle to define the role that multiscale interactions (e.g., cumulus, mesoscale, synoptic, planetary) might play in the manifestation of the ISO as well the degree and manner that cloud–radiative interactions might be important. While the land surface is an inherent part of the geographic extent of the boreal summer ISO, very little research has been performed to evaluate its role. In addition, there are clearly some very general numerical simulation problems that still need to be overcome that when solved will have a positive impact on the simulation of ISV. These include better mean states, undoubtedly the treatment of convection including the roles of stratiform/anvil clouds and shallow cumulus, when and where ocean coupling is important, etc. Finally, while the development and application of

empirical ISO forecast models is taking foot, the ability to exploit the details associated with a weather/climate prediction GCM is at best in its infancy. At this stage there are not only the difficulties associated with the simulation of ISV, there are still many uncertainties associated with how to carry out subseasonal predictions in terms of supplying initial conditions and supplying/modeling surface boundary conditions (Waliser *et al.*, 2003a). The development and improvement of subseasonal predictions, based on phenomena such as the ISO, offer a great opportunity to help bridge the present gap between weather and seasonal-to-interannual climate predictions.

5.9 ACKNOWLEDGEMENTS

This work was supported by the Human Resources Development Fund at the Jet Propulsion Laboratory, as well as the National Science Foundation (ATM-0094416), the National Oceanographic and Atmospheric Administration (NA16GP2021), and the National Atmospheric and Aeronautics Administration (NAG5-11033). The author would like to thank an anonymous reviewer and the editor for providing a number of useful comments and suggestions that improved the balance of material in this chapter along with its presentation. The author would also like to thank D. R. Chakraborty for contributing material for the section on Theory and Physical Processes.